Smoke Control by Mechanical Exhaust or Natural Venting

51

James A. Milke

Introduction

Smoke management in large-volume spaces, such as atria and covered malls, poses separate and distinct challenges from well-compartmented spaces. In particular, smoke control strategies using pressure differences and physical barriers described by Klote in Chap. 50, and NFPA 92, *Standard for Smoke-Control Systems* [1], are infeasible. Without physical barriers, smoke propagation is unimpeded, spreading easily throughout the entire space. The tall ceiling heights in many large-volume spaces pose additional challenges because of the production of substantial quantities of smoke and delayed detection times. However, on the positive side, the combination of large-volume space and tall ceiling height permit the smoke to become diluted and cooled as it spreads vertically and horizontally, thereby reducing the level of hazard posed by the smoke. Even so, there is still a need to ensure that dangerous concentrations of smoke are prevented in large-volume spaces.

In addition to atria and covered malls, there are many other examples of large-volume spaces, including convention centers, airport terminals, sports arenas, and warehouses where smoke management is of concern. The engineering principles governing the design of smoke control systems for all of these various large-volume spaces are the same. However, differences in the smoke control system designs for the variety of large-volume spaces may be found. Differences in designs are a result of differences in fire scenarios and design goals, reflecting the range of building uses and operations and the nature of who or what may be exposed to the smoke. Given the similarities in engineering principles affecting smoke control system design, the term *atrium* will be used throughout this chapter to refer to all types of large-volume spaces.

The discussion presented in this chapter is divided into two sections. First, conditions within the atrium prior to actuation of a smoke control system are discussed. As part of this discussion, the smoke filling process is described along with the time required for actuation of a smoke control system. The second part of the chapter includes a description of conditions within the atrium after actuation of the smoke control system.

As a preface to any discussion on smoke control systems, a definition of smoke must be established (NFPA 92, *Standard for Smoke Control Systems* [1], Section 3.3.13):

> The airborne solid and liquid particulates and gases evolved when a material undergoes pyrolysis or combustion, together with the quantity of air that is entrained or otherwise mixed into the mass.

Although only the combustion products are visible and potentially toxic, what is visually observed as smoke is a mixture of the combustion products and the entrained air. Air is

J.A. Milke (✉)
University of Maryland, Department of Fire Protection Engineering, University of Maryland, College Park, MD, 20742, USA

M.J. Hurley (ed.), *SFPE Handbook of Fire Protection Engineering*,
DOI 10.1007/978-1-4939-2565-0_51,

entrained along the entire height of the smoke plume below a smoke layer. Proportionally, the smoke is mostly entrained air. In the space between the base and tip of the flames, most of the entrained air is not consumed in the combustion process and only dilutes the combustion products. Entraining air into the smoke plume increases the mass flow in the plume to increase the quantity of smoke produced. However, the entrained air also dilutes the smoke to decrease the concentration of combustion gases and cool the smoke. In some cases, the smoke may be sufficiently diluted to mitigate the associated hazards.

Hazard Parameters

Smoke can adversely affect building occupants, fire brigade members, property (including the building structure and contents), and mission continuity. Typically, the threat to people or objects is posed when they come into contact with smoke for a sufficient period of time.

People who become exposed to smoke are generally harmed as a result of the exposure to toxic gases or elevated temperature. The toxic effects of smoke on people are described in Purser (see Chap. 63) and Klote et al. [2]. In addition, smoke may reduce visibility. A reduction of visibility may cause people to become disoriented and can in turn increase the amount of time they are exposed to the smoke [3]. A reduction of visibility may also increase the susceptibility of building occupants to trip over obstructions or even fall over balcony railings [4].

Building components can be affected by the elevated temperature due to smoke. Building components heated by smoke are considered in fire resistance analyses. In addition, building contents may be affected by exposure to the elevated temperatures, corrosive gases, or particulate matter. Contents exposed to heated smoke may be melted, distorted, or charred, depending on the temperature of the smoke and the degree of exposure. Contents that are submerged in smoke and come into contact with combustion gases and smoke particles may become stained or emit an odor of smoke. Exposure to smoke can damage electronic equipment, especially if restoration activities are not initiated promptly after the fire [5].

Following a fire, a building or portion thereof may be closed due to restoration, threatening mission continuity. This results in loss of revenue for the building owner, temporary unemployment of workers in the building, and loss of service of the facility to the community, among other outcomes.

Smoke Layer Interface Position

The smoke layer interface position is located a distance, z, above the top of the fuel, as indicated in Fig. 51.1. This parameter is used to assess the danger of people or objects being immersed in a smoke layer. Sole use of this parameter to assess hazard level is conservative by considering any concentration of smoke to be unacceptable. For people, even though the physiological effects due to being submerged in "light" smoke levels may be minor, the psychological effects and extended evacuation time may be appreciable. Being surrounded by smoke of any nature may decrease the speed of evacuation, perhaps until the smoke is no longer relatively benign. In terms of property protection issues, any smoke may be unacceptable because of smoke staining or smoke corrosivity.

Light Obscuration

As with the smoke layer depth parameter, light obscuration is not lethal by itself. Associated with an increase in light obscuration is a reduction in visibility, which is likely to yield a longer evacuation time and extend exposure to the toxins in smoke. In some documented fires, evacuation has been terminated due to a lack of sufficient visibility [6–8]. A fire fighter's injury in an atrium fire was attributed to a significant

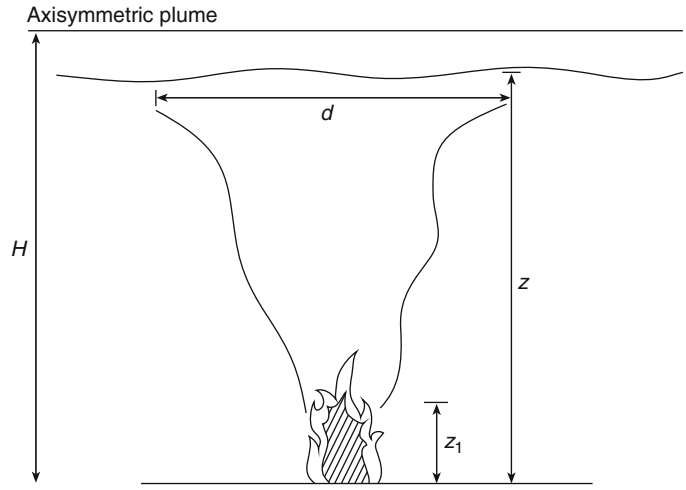

Fig. 51.1 Axisymmetric plume [1]

reduction in visibility due to light obscuration [4]. The fire fighter fell from an upper balcony because he could not see the edge.

Limiting values from 0.23 to 1.2 m^{-1} have been suggested for the extinction coefficient [6–8]. Alternatively, a critical limit may be based on a preferred minimum visibility distance to a particular target. For example, a limit of light obscuration can be suggested such that occupants can see an illuminated exit sign across a room or at the end of a corridor [3, 9].

Temperature and Gas Specie Concentration

The final two parameters, elevated temperature of the smoke layer and gas specie concentration (such as CO, CO_2, and HCN), can be directly related to the potential for harm (see Chap. 63). Critical limits for these two parameters can be suggested based on toxicity studies.

Smoke Management Approaches

The design of a smoke control system for an atrium is influenced by the following three characteristics of the atrium:

1. Geometric shape and dimensions
2. Relative location within the building
3. Separation from communicating spaces

Several approaches are available to achieve smoke management goals in an atrium (e.g., limit the fire size, provide physical barriers, and provide mechanical or natural ventilation). Selection of the best smoke management approach for a particular atrium should consider the use, size, and arrangement of the associated spaces.

Limiting the fire size can be accomplished by controlling the type, quantity, and arrangement of fuel. In addition, the fire size can be controlled through an automatic suppression system.

Physical barriers limit smoke spread to adjacent spaces. The ability of a physical barrier to limit smoke spread is dependent on the leakage of the barrier and pressure difference across the barrier. The barrier needs to withstand the exposure to smoke and an elevated temperature environment. In an atrium with a tall ceiling, the temperature of the smoke layer in the atrium may be only slightly above ambient temperatures in the space.

Mechanical or natural ventilation may be provided to remove smoke from the atrium. Removing smoke from the atrium can be intended to limit the accumulation of heat and smoke within the atrium or arrest the descent of the smoke layer. Mechanical ventilation can be provided to oppose smoke movement induced by the fire to restrict smoke spread to communicating

spaces. Gravity vents may be provided to remove smoke, though their performance can be compromised by environmental factors.

Analytical Approach

Numerous tools are available to aid in the design and evaluate the adequacy of a smoke control system. The selection of a particular tool is dependent on the accuracy needed for the analysis and the applicability of the analytical tools given the characteristics of the large space and selected fire scenarios. The principal characteristics that affect applicability are

- Geometry of the large space: variation of horizontal cross-sectional area, sloped versus flat ceiling
- Transient aspects: unsteady versus steady heat release rate, constant versus transient operation of smoke control system
- Fire development: heat release rate as a function of time (for example, constant, power-law relationship with time, t^n)
- Environmental effects: stack effect, wind
- Interacting systems: other smoke control systems, HVAC, other exhaust systems (for example in laboratories)

The range of design tools available to assess the performance of smoke control system designs can be grouped into the following categories:

- Zone model (algebraic equation based)
- Zone model (computer based)
- Field model
- Physical scale model

The intent of an engineering analysis of smoke conditions in an atrium is to express the level of hazard in terms of physically based parameters, for example, smoke layer interface position, temperature, gas concentration (such as carbon monoxide), and light obscuration. The magnitude of each of these parameters can be predicted based on engineering principles. In addition to being predictable, critical threshold values are available for the hazard parameters in order to properly assess the severity of the threat (See Chap. 63). This chapter will concentrate on the life hazards posed by smoke. The hazards smoke poses to contents, property, and mission continuity are described elsewhere [2–4, 10].

Physical Scale Models

Physical scale models provide a representation of a space, though in a reduced scale. Physical scale models are especially useful in examining atria with irregular shapes or numerous projections. A review of applying physical scale models as a design aid for atrium smoke control systems was provided by Milke and Klote [11].

Quintiere provided a review of scaling relationships based on preserving the Froude number [12]. The Froude number, Fr, is defined as v/gl.

The scaling relations are

Temperature:

$$T_m = T_F \tag{51.1}$$

Geometric position:

$$x_m = x_F \left(\frac{l_m}{l_F}\right) \tag{51.2}$$

Pressure:

$$\Delta p_m = \Delta p_F \left(\frac{l_m}{l_F}\right) \tag{51.3}$$

Velocity:

$$v_m = v_F \left(\frac{l_m}{l_F}\right)^{1/2} \tag{51.4}$$

Time:

$$t_m = t_F \left(\frac{l_m}{l_F}\right)^{1/2} \tag{51.5}$$

Convectiveheat release:

$$\dot{Q}_{c,m} = \dot{Q}_{c,f} \left(\frac{l_m}{l_F}\right)^{5/2} \tag{51.6}$$

Volumetric flow rate:

$$V_{\text{fan},m} = V_{\text{fan},F} \left(\frac{l_m}{l_F}\right)^{5/2} \tag{51.7}$$

Experiments based on Froude modeling may be done with air at atmospheric pressure. Froude modeling does not preserve the Reynolds number. However, appropriate selection of the size of the physical scale model can ensure that fully

developed flow is achieved to minimize the consequences of not preserving the Reynolds number. Because the smoke behavior in only certain areas of the scaled atrium may be of interest, fully developed flow only needs to be achieved in these particular areas. Often a physical scale model with a critical dimension of at least 0.3 m in any areas of interest will be sufficient to achieve fully developed, turbulent flow. As an example, in most shopping malls and atria, the critical dimension in question would be the floor-to-ceiling height of one of the balconies.

In addition, Froude modeling does not preserve the dimensionless parameters concerning heat transfer. Generally, this limitation has little effect because the temperature is the same for the physical scale model and the full-scale facility. Froude modeling does not apply to locations with high temperature and low Reynolds numbers (e.g., near the flame). However, Froude modeling provides useful information about smoke transport away from the fire.

Some surface effects can be preserved by scaling the thermal properties of the construction materials for the model. The thermal properties can be scaled by

Thermal properties:

$$\left(k\rho c_p\right)_{w,m} = \left(k\rho c_p\right)_{w,F}\left(\frac{l_m}{l_F}\right)^{0.9} \qquad (51.8)$$

Because scaling thermal properties have only a secondary effect on fluid flow, considerations of convenient construction and flow visualization may require that some or all surface materials in the model are different from those selected based on thermal property scaling.

Example 1 A physical scale model is proposed to determine the equilibrium smoke layer position for the atrium depicted in Fig. 51.2. Because the horizontal cross-sectional area varies with height, algebraic equation and computer-based zone models are of limited value. The overall height of the atrium being studied is 30.5 m and the design fire is steady with a heat release rate of 5 MW. An exhaust fan capacity of 142 m^3/s is proposed. By applying the scaling relationships

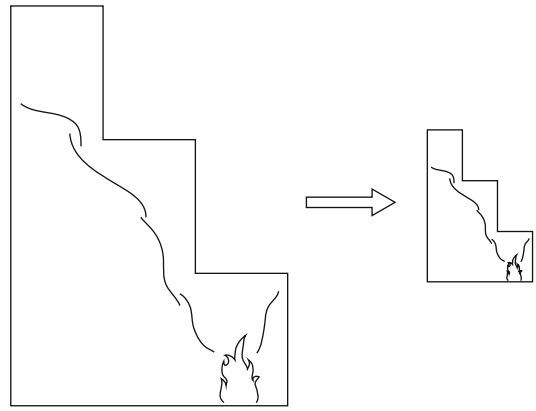

Fig. 51.2 Small-scale model of atrium

to formulate a small-scale model, the basic parameters for the scale model are

- Height: 3.8-m-tall model (1/8 scale)
- Fire size: 28 kW
- Fan capacity: 0.78 m^3/s

Analytical Models

Two categories of analytical models are zone and field models. A description of field models is outside the scope of this chapter. Zone models divide each compartment into a limited number of control volumes, typically an upper and a lower zone. Inherent in the zone approach is the assumption of uniform properties throughout each zone. In spaces with a large floor area, this assumption may be tenuous. Nonetheless, calculations associated with the zone model approach are relatively easy to perform and are often accepted for engineering purposes. Calculations following the zone model approach may be in the form of algebraic equations or a computer algorithm.

The zone model approach assumes that smoke from a fire is buoyant, rises to the ceiling, and forms a smoke layer. The buoyant nature of smoke is due to the decreased density of the heated smoke. As smoke rises in a plume, air is entrained to increase the mass flow rate in the plume. A decrease in the velocity and temperature of the smoke plume results from the increase in the plume mass flow rate, as dictated by

conservation of momentum and energy. In addition, the entrained air dilutes the combustion products in the plume. The entire smoke layer is assumed to have uniform characteristics. As smoke is supplied to the smoke layer from the plume, the interface between the smoke layer and lower clear air zone descends. The additional smoke supplied by the plume also results in an increase in the smoke layer temperature, carbon monoxide concentration, and light obscuration.

Being a simplification, the zone model approach may not be applicable in some situations. One example includes a scenario with operating sprinklers, which may cool the layer and also entrain smoke from the upper layer into the water spray pattern descending into the lower zone. Another example consists of the case where smoke does not reach the ceiling as a result of a loss of buoyancy, where the pre-fire temperature near the ceiling of the atrium is greater than that near the floor. This situation is discussed in more detail later in this chapter. A third situation involves an atrium with a large cross-sectional area where the horizontal variation in conditions from one portion of the atrium to another is important to the analyst. Where localized conditions associated with the smoke plume or smoke layer need to be assessed, field models are more appropriate than zone models.

Two categories of fire scenarios for smoke management design in atria include (1) fires located in the atrium, and (2) fires located in a space adjacent and open to the atrium. This chapter concentrates only on fires within the atrium space. Methods to estimate conditions in any of the adjacent spaces, resulting from fires originating in the atrium or from fires in other adjacent spaces, are addressed elsewhere [2].

Smoke Filling Period

A smoke layer is formed once the smoke plume reaches the ceiling and the ceiling jet spreads horizontally to reach the bounding walls of the space. Subsequently, the smoke layer starts to descend in the space. In relatively small spaces with low ceilings, the smoke layer forms almost immediately. However, in large spaces with tall ceilings, the time required to form a smoke layer may be appreciable. The delay in forming a layer is attributable to the transport lag of the smoke. The smoke filling period continues until the properly sized smoke exhaust fans are actuated.

Transport Lag

The transport lag is composed of the time for a smoke plume to reach the ceiling (plume transport lag) and the time for the ceiling jet to reach the bounding enclosure (ceiling jet transport lag). These two time periods are depicted in Fig. 51.3.

Correlations for the plume and ceiling jet transport lag are available in the literature for both steady and t^2 fires [13, 14]. Because virtually all fires have a growth period before reaching a steady phase, the transport lag correlations for steady fires have little relevance.

Correlations for the plume transport lag for steady and t^2-fires are
Steady files:

$$t_{pl} = 0.67H^{4/3}/\dot{Q}^{1/3} \tag{51.9}$$

t^2 fires:

$$t_{\mathrm{pl}} = 0.1H^{4/5}t_g^{2/5} \tag{51.10}$$

Estimates of the plume transport lag from Equations 51.9 and 51.10 are provided in Fig. 51.4. As indicated in the figure, even the shortest plume transport lag for t^2 fires, associated with the fast t^2 fire, is greater than that for a modest-size steady fire.

Comparable correlations for the ceiling jet transport lag for steady and t^2 fires are
Steady files:

$$t_{\mathrm{cj}} = \frac{r^{11/6}}{1.2\dot{Q}^{1/3}H^{1/2}} \tag{51.11}$$

t^2 fires:

$$t_{\mathrm{cj}} = \frac{0.72rt_g^{2/5}}{H^{1/5}} \tag{51.12}$$

A comparison of the ceiling jet transport lag for a modest-size steady fire and t^2 fires is

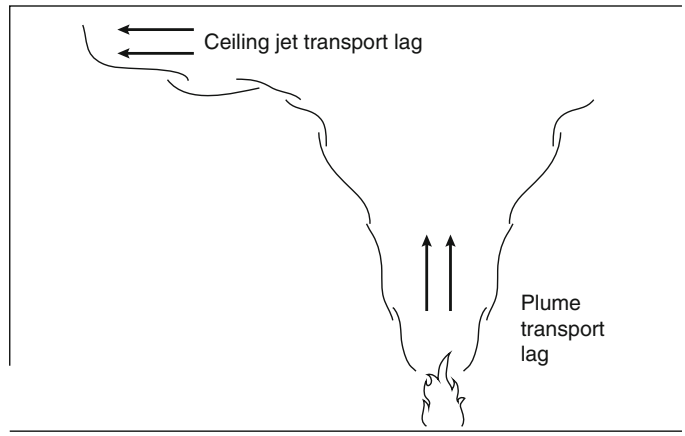

Fig. 51.3 Plume and ceiling jet transport lag

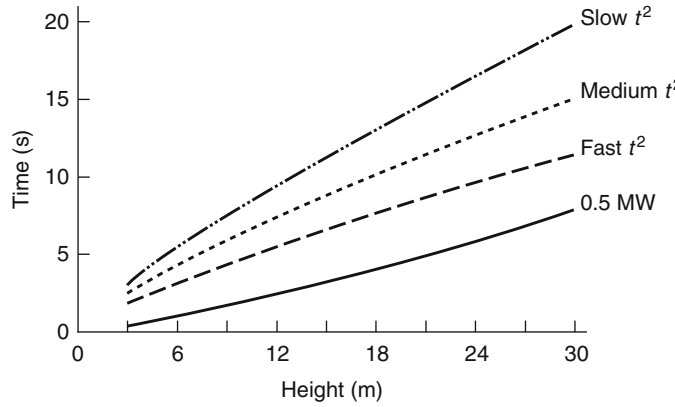

Fig. 51.4 Plume transport lag

presented in Fig. 51.5. Again, the transport lag associated with the steady fire is much less than that associated with any of the t^2 fires.

Many zone models do not account for transport lag. In low-height spaces with small compartments, this is likely to be inconsequential. In tall spaces with large cross-sectional horizontal areas, the lag may be important. In such cases, only models that incorporate transport lag are to be selected.

Smoke Layer Interface Position

Once the smoke layer has formed, the initial rate of descent of the layer is very rapid, slowing as the layer descends. This is attributable to the rate of smoke production being dependent on the height of the plume where entrainment occurs, i.e., the distance from the top of the fuel to the smoke layer.

Both empirical correlations and theoretically based methods are available to address conditions during the smoke filling period using a zone model approach [15]. Theoretically based methods use statements of conservation of mass and energy to determine the volume of the upper layer. Conservation of mass accounts for the smoke mass supplied from the plume to the smoke layer along with any smoke leaving the zone through ventilation openings. Conservation of energy is applied to address the energy being supplied by the plume along with heat losses from the layer.

Generally, the predicted smoke layer interface position determined by the two analytical

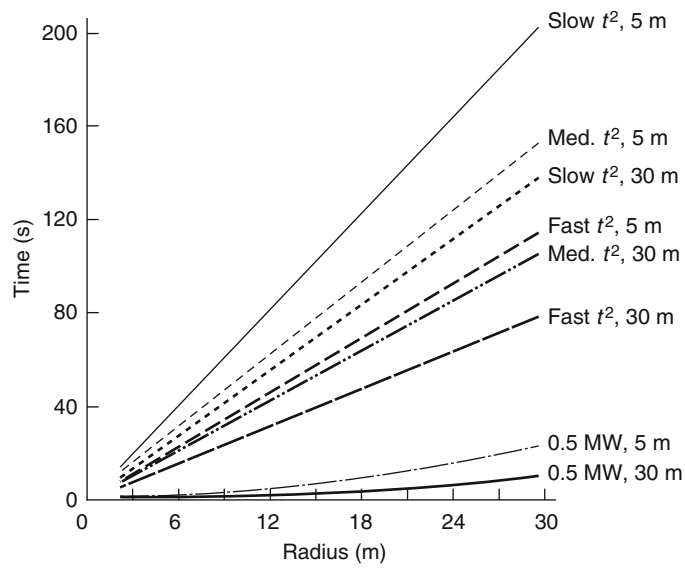

Fig. 51.5 Ceiling jet transport lag

methods differs. The smoke layer is comprised of the uppermost portion of the layer in which the conditions are relatively uniform at any elevation. Below that section is a transition zone, where the conditions decrease until they reach the bottom edge of the layer and are at their minimum value. The predictions from the empirical correlations relate to the position of the bottom edge of the transition zone as determined in an experimental program. In the theoretically based correlations, all of the smoke is considered to be in one layer with uniform properties. Combination of the transition zone and the upper portion into one uniform zone effectively results in the transition zone being compressed so as to have the same properties as the upper portion. As such, the theoretically based correlations relate to a thinner smoke layer than the empirical approach.

Empirical Correlations

Empirical correlations have been developed by Heskestad to determine the smoke layer interface position as a function of time for steady and t^2 fires. These correlations, included in NFPA 92 [1], are based on experimental data in large spaces. In the experimental efforts, the smoke layer interface position was established by a variety of means, including visual observations and measurements of temperature change, carbon dioxide concentration, or light obscuration.

The correlations are simple expressions with easily acquired input and minimal computations. The correlations provide conservative estimates of the smoke layer interface position (i.e., predicting the lower edge of the transition zone of the smoke layer which may include only 'wisps' of smoke) [16]. The correlations are applicable to simplified cases related to the fire and geometry of the space. Fire scenarios must be steady state or, if growing, follow a t^2 profile. The assumed geometrical configuration is a space of uniform cross-sectional area (i.e., rectangular or right cylindrical solids). In addition to the noted simplifications, second-order parameters such as environmental factors (e.g., stack effect, wind) and the effect of HVAC systems are neglected.

Steady Fires The position of the smoke layer interface for steady fires can be estimated using Equation 51.13 [16, 17]. Equation 51.13 is based on experimental data from fires in large-volume spaces with A/H^2 of 0.9–14 [18–20].

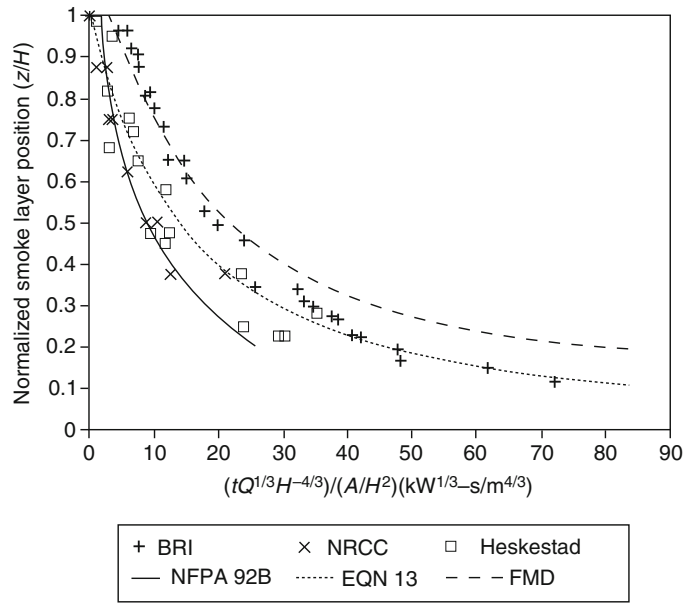

Fig. 51.6 Comparisons of smoke layer position—experimental data versus predictions

$$\frac{z}{H} = 1.11 - 0.28 \ln\left(\frac{t\dot{Q}^{1/3}H^{-4/3}}{A/H^2}\right) \qquad (51.13)$$

Where $z/H \geq 0.2$.

Equation 51.13 is presented in non-dimensional form. The quantity $t\dot{Q}^{1/3}H^{-4/3}$ represents the normalized time from ignition. The significance of the normalized time parameter is to indicate that the same relative smoke layer position occurs for a long duration, low heat release rate fire in a tall ceiling height atrium, as for a short duration, large fire in an atrium with a short ceiling height. Different atrium geometries are accounted for by the non-dimensional shape factor, (A/H^2) [18, 19].

The limits noted for A/H^2 reflect the range of shape factors for the facilities in which the experiments were performed [18, 19]. Examples of atria within the noted range include atria with a cross-sectional area of 10,000 m^2 and a height of 105 m ($A/H^2 = 0.9$) or a height of 27 m ($A/H^2 = 14$). Comparisons of the predictions from Equation 51.13 to experimental data from fires in tall spaces are provided in Fig. 51.6 [20–22].

Transport lag, or the initial time period to form a smoke layer, is implicitly included in Equation 51.13. Evidence of this characteristic is obtained for short time durations where the resulting z/H is greater than 1.0 (otherwise $z/H > 1$ would literally mean that the smoke layer interface is *above* the ceiling). The lower limit for z/H of 0.2 relates to the lowest level where data were taken in any of the referenced experiments.

t^2fires Equation 51.14 provides a correlation of the time-dependent smoke layer interface position for fires following a t^2-type profile [16]. Equation 51.14 is also based on experimental data in spaces with shape factors ranging from 0.9 to 14 [20, 23].

$$\frac{z}{H} = 0.91\left[tt_g^{-2/5}H^{-4/5}\left(A/H^2\right)^{-3/5}\right]^{-1.45} \qquad (51.14)$$

Equations 51.13 and 51.14 both assume that the fire is located near the center of the atrium floor, remote from any walls. Smoke production is greatest for the centered configuration and thereby represents the worst-case condition.

Example 2 For a fast, t^2 fire in an atrium with a cross-sectional area of 800 m^2 and height of 20 m, determine the position of the smoke layer interface after 120 s.

Solution Applying Equation 51.14 with $A/H^2 = 2.0$ and $t_g = 150$ s, z/H is 0.95 or $z = 19$ m.

Example 3 For a fast, t^2 fire in an atrium with a cross-sectional area of 800 m^2 and height of 20 m, determine the time for the smoke layer interface to reach 15 m above floor level.

Solution Re-expressing Equation 51.14 to solve for t,

$$t = 0.94 t_g^{2/5} H^{4/5} \left(A/H^2\right)^{3/5} (z/H)^{-0.69} \quad (51.15)$$

Applying Equation 51.15 with $A/H^2 = 2.0$ and $t_g = 150$ s, t is 140 s.

Reviewing the results from Examples 2 and 3, the smoke layer barely descends below the ceiling in the first 120 s. This is indicative of the lag time required for the plume to reach the ceiling and to form a layer. Then, after only another 20 s, the smoke layer descends 4 m, demonstrating the rapid initial descent rate of the smoke layer interface. The rapid descent is attributable to the significant quantity of smoke produced during the early stage of a fire in a tall ceiling space when the height available for entrainment is at its largest value. The predicted trend of rapid filling during the early stage of a fire has been reported by eye-witness accounts from four fires in atria [4, 24–26].

Theoretically Based Approach

Conservation of mass and energy can be applied to provide an estimate for the position of the theoretical smoke layer interface. Equation 51.16 expresses the conservation of mass, m_u, for the upper smoke layer, assuming no exhaust from the layer.

$$\frac{dm_u}{dt} = \dot{m} \quad (51.16)$$

Approximating the smoke as an ideal gas with properties of heated air, and assuming that the ambient pressure and specific heat are constant, the expression for conservation of energy for the smoke layer is

$$(\rho h)_u \frac{dV_u}{dt} = \dot{Q}_c + \dot{m} h_1 \quad (51.17)$$

Given the previously assumed conditions, ρh is a constant. Substituting the volumetric flow rate for the mass flow rate and simplifying,

$$\frac{dV_u}{dt} = \frac{\dot{Q}_c}{\rho h} + \dot{V} \quad (51.18)$$

The growth rate of the upper layer indicated in Equation 51.18 is dependent on two terms: (1) the volume supplied by the plume and (2) the expansion of the volume due to heating. For the case of an atrium with a constant cross-sectional area, A,

$$\frac{dV_u}{dt} = A \frac{dz_u}{dt} \quad (51.19)$$

As long as the smoke layer interface is well above the flaming region (see discussion later in this chapter), the plume mass entrainment rate can be estimated from [27].

$$\frac{dV_u}{dt} = \frac{\dot{m}}{\rho} = k_v \dot{Q}^{1/3} z^{5/3} \quad (51.20)$$

Several simplifications can be made for large clear heights (i.e., clear heights in excess of 10 m). The clear height is the distance from the top of the fuel to the bottom of the smoke layer. The magnitude of the second term is much less than the first. Generally, z is much greater than z_o. In addition, the volume increase of the upper layer supplied by the plume is appreciably greater than that due to expansion. With these simplifications and by substituting Equations 51.19 and 51.20 into Equation 51.18, an expression for dz_u/dt can be formulated

$$\frac{dz_u}{dt} = \frac{k_v \dot{Q} z^{5/3}}{A} \quad (51.21)$$

In Equation 51.21, k_v is the volumetric entrainment constant, defined as [36].

$$k_v = 0.076/\rho$$

The convective heat release fraction is the ratio of the convective heat release rate to the total heat release rate and is typically assumed

to be on the order of 0.7–0.8. Throughout this chapter, a value of 0.7 is selected for the convective heat release fraction [1]. Assuming a plume entrainment constant of 0.076 kg $kW^{-1/3} \cdot m^{-5/3} \cdot s^{-1}$ and the density of ambient air as 1.2 kg/m^3, the volumetric entrainment constant is 0.064 $m^{4/3}$ $kW^{-1/3}$ s^{-1}.

An expression for the smoke layer position resulting from a steady fire as a function of time can be obtained by integrating Equation 51.9:

$$\frac{z}{H} = \left[1 + \frac{2k_v t \dot{Q}^{1/3}}{3(A/H^2)H^{4/3}}\right]^{-3/2} \tag{51.22}$$

Alternatively, for a t^2 fire

$$\frac{z}{H} = \left[1 + \frac{4k_v t(t/t_g)^{2/3}}{(A/H^2)H^{4/3}}\right]^{-3/2} \tag{51.23}$$

A comparison of the predictions from Equations 51.13 and 51.22 is provided in Fig. 51.6. One principal difference relates to the time delay for the smoke layer to form, i.e., transport lag. Transport lag is included implicitly in Equation 51.13. Equation 51.22 assumes that a smoke layer forms immediately. The transport lag can be accounted for separately [13].

Example 4 For a fast, t^2 fire in an atrium with a cross-sectional area of 800 m^2 and height of 20 m, determine the position of the smoke layer interface after 120 s.

Solution Applying Equation 51.23 with $A/H^2 = 2.0$ and $t_g = 150$ s, z/H is 0.72 or $z = 14.4$ m.

Vented Period

If a smoke control system has the capability to exhaust smoke, the descent of the smoke layer can be arrested if the volumetric rate of smoke exhaust from the smoke layer equals the volumetric rate of smoke supplied to the layer. Neglecting the effect of expansion, the layer descent is stopped when the mass exhaust rate is equal to the mass entrainment rate by the plume. Algebraic equations are available to estimate the properties of the smoke layer, including

1. Position of smoke layer interface
2. Temperature of smoke layer
3. Light obscuration in smoke layer and
4. Gas concentration in smoke layer

Equilibrium Smoke Layer Interface Position

The exhaust rate necessary to arrest the descent of the smoke layer can be estimated based on knowledge of the mass entrainment rate into the plume. The mass entrainment rate depends on the configuration of the plume. Plume configurations reviewed in this chapter are

1. Axisymmetric plume
2. Wall plume
3. Corner plume
4. Balcony spill plume

Axisymmetric Plume Axisymmetric plumes are formed from fires involving fuel packages remote from any walls (i.e., near the center of the atrium floor). Being remote from any walls, air is entrained around all of the plume perimeter along the entire clear height of the plume. The functional relationship of the mass entrainment rate to the heat release rate and clear height is [28].

$$\dot{m} = f\left(\dot{Q}_c^{1/3} z^{5/3}\right) \tag{51.24}$$

One set of equations for the mass entrainment rate was originally derived by Heskestad [27]. One of the equations in the pair developed by Heskestad applies to estimating the entrainment in the flaming portion of the plume and another deals with the overall plume, including flaming portion and upper portion where flames are absent.

The limiting height is defined as the height of the continuous flaming region, (i.e., where flames are present 50 % of the time). The limiting height may be estimated as [27].

$$z_f = 0.166\dot{Q}_c^{2/5} \tag{51.25}$$

For clear heights less than the limiting height, i.e., where flames extend into the smoke layer, the entrainment rate is estimated using Equation 51.26

$$\dot{m} = 0.032\dot{Q}_c^{3/5} z \tag{51.26}$$

For clear heights greater than the limiting height, i.e., where the flaming region ends prior to reaching the smoke layer, the entrainment rate is estimated using Equation 51.27:

$$\dot{m} = 0.071\dot{Q}_c^{1/3} z^{5/3} + 0.0018\dot{Q}_c \tag{51.27}$$

Equation 51.27 is a simplified version of the original expression developed by Heskestad (see Chap. 13, with z_o from the original expression set equal to zero. The validity of neglecting z_o in Equation 51.27 is based on the observation that z_o is typically small, compared to z [2]. The location of the virtual origin of an assumed point source can be estimated as [27].

$$z_o = 0.083\dot{Q}^{2/5} - 1.02d_o \tag{51.28}$$

For noncircular fuels, an equivalent diameter needs to be defined. The definition of an equivalent diameter is based on a circle that has an area equal to the floor area covered by the fuel. Considering a wide range of diameters and heat release rates associated with a variety of typical fuel packages, the virtual origin ranges from 0.5 to −5 m. Negative values are obtained when the second term is greater than the first (i.e., for fuel commodities with modest heat release rates spread over a large area).

Originally, Equations 51.26 and 51.27 were developed to describe plumes from horizontal, circular flammable liquid pool fires. However, these equations have been shown to be applicable to more complex fuels, as long as the limiting height is greater than the diameter of the fuel, and the fire only involves the surface of the material (i.e., is not deep-seated) [27].

The mass rate of smoke production estimated by Equations 51.26 and 51.27 is independent of the type of materials involved in the fire, other than indirectly in terms of the heat release rate. This is due to the mass rate of entrained air being much greater than the mass rate of combustion products generated, which is true as long as sufficient air is available for combustion. As a result of the fire being approximated as a point source in the entrainment equations, the shape or form of the fuel is not of primary importance. Thus, the parameters associated with a detailed description of the fuel package are relegated to a level of secondary importance.

In both Equations 51.26 and 51.27, the mass entrainment rate is dependent on the clear height, where the mass entrainment rate increases with increasing values of the clear height. During the early stages of the fire, the clear height has its maximum value thereby providing the maximum smoke production rate. This is especially true if the flame height is well below the smoke layer, where the smoke production rate is proportional to $z^{5/3}$.

In most engineering applications, the smoke production (or exhaust) rate is expressed in terms of a volumetric rate rather than a mass rate. In order to accommodate this preference, the relationship between the volumetric rate and mass rate is expressed as Equation 51.29.

$$\dot{V} = \frac{\dot{m}}{\rho} \tag{51.29}$$

Assuming smoke to have the same properties as air, the density of smoke may be evaluated as the density of air at the temperature of the smoke layer [3]. Graphs relating the volumetric smoke production rate to the clear height for selected total heat release rates ranging from 1000 to 10,000 kW are provided in Fig. 51.7.

Example 5 A fire has a total heat release rate of 5000 kW and is located at the center of the atrium floor. The smoke layer interface is 35 m above the floor. Determine the mass and volumetric rates of smoke being supplied by the plume to the smoke layer (i.e., at the location of the smoke layer interface).

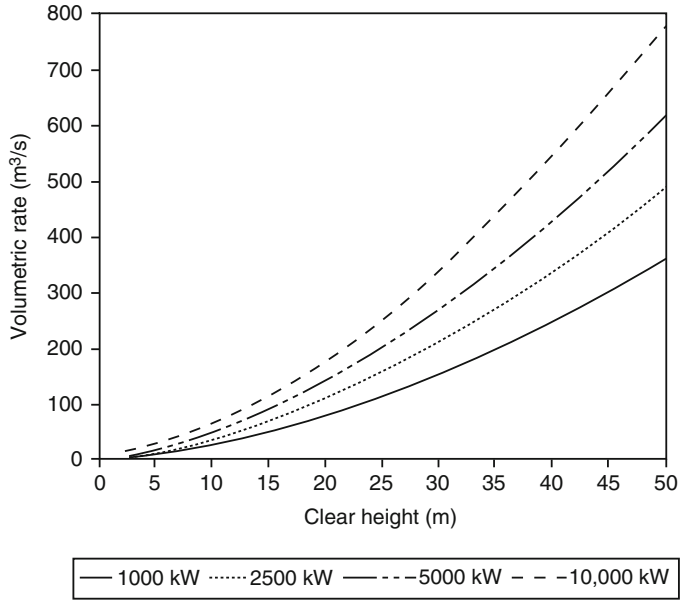

Fig. 51.7 Smoke production rate for axisymmetric plumes

Solution First, the limiting height is evaluated using Equation 51.25 to determine the applicable equation for the mass rate of entrainment, assuming the convective heat release fraction is 0.7, $z_f = 4.3$ m. Because z > z_f, Equation 51.27 is the applicable equation for determining the mass rate of smoke production. Neglecting z_o, the mass smoke production rate is 410 kg/s. The associated volumetric rate (from Equation 51.29, assuming 20 °C and 1 atm pressure) is 340 m^3/s.

Wall and Corner Plumes Fires located near walls and corners principally entrain air only along the surface of the plume away from the walls or corner. Consequently, the amount of smoke production is reduced for these locations, compared to the axisymmetric plume remotely located from the walls. Using the concept of reflection, the smoke production rate from wall and corner plumes can be estimated [29, 30].

A plume generated by a fire located against a wall only entrains air from approximately half of its perimeter, as indicated in Fig. 51.8. According to the concept of reflection, the smoke production rate is estimated as half of that from a fire that is twice as large (in terms of heat release rate) (note: having half of the entrainment does not cancel out the impact of considering twice the fire size as the entrainment is proportional to the one-third power of the heat release rate).

Similarly, a plume generated by a fire located near a corner of a room is referred to as a corner plume (see Fig. 51.8). Using the concept of a reflection, the smoke production rate from corner plumes, where the intersecting walls form a 90° angle, is estimated as one-quarter of that from a fire that is four times as large.

Example 6 A fire located on the floor of an atrium has a total heat release rate of 5000 kW. The smoke layer interface is 35 m above the floor. Compare the mass rates of smoke being supplied by the plume to the smoke layer, given an axisymmetric, wall, or corner plume configuration.

Solution In Example 5, $z_f = 4.3$ m and the smoke production rate for the axisymmetric plume using Equation 51.27 is 410 kg/s. Applying the same equation for the wall plume, the smoke production rate for a fire size of 10,000 kW is estimated as 520 kg/s. Dividing that rate by two provides the smoke production rate for the wall plume (260 kg/s). Similarly, for

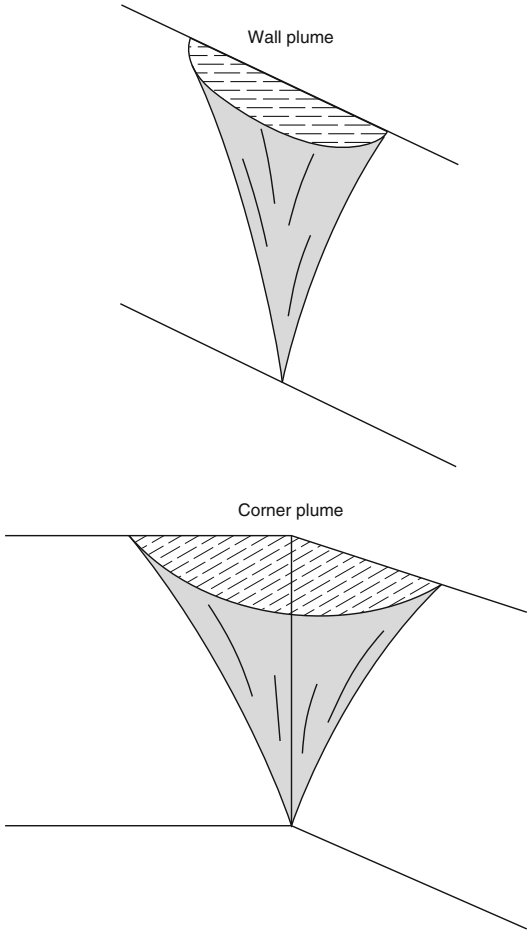

Fig. 51.8 Wall and corner plume diagrams

the case of the corner plume, the smoke production rate is 170 kg/s (considering one-quarter of the smoke production rate from a 20,000 kW fire).

Comparing the smoke production rates for the three plumes (axisymmetric, wall, and corner plumes), the smoke production rate is greatest for the axisymmetric plume (410 kg/s) compared to 260 and 170 kg/s for the wall and corner plumes, respectively. Thus, conservative hazard assessments should assume an axisymmetric plume is developed from a fire that is located away from the walls, near the center of the space.

Balcony Spill Plume A balcony spill plume is generated in cases where smoke reaches an intermediate obstruction, such as a balcony, travels horizontally under the obstruction, and then turns and rises vertically. Scenarios with balcony spill plumes involve smoke rising above a fire, reaching a ceiling, balcony, or other significant horizontal projection, then traveling horizontally toward the edge of the balcony. Characteristics of the resulting balcony spill plume depend on characteristics of the fire, width of the spill plume, and height of the ceiling above the fire. In addition, the path of horizontal travel from the plume centerline to the balcony edge is significant.

Several correlations on air entrainment into balcony spill plumes have been presented in the literature over several decades. A comprehensive review of the proposed correlations is provided by Harrison [31], Lougheed et al. [32] and Lim [33]. The correlations presented in NFPA 92 reflect the results obtained by Lougheed et al. from large-scale experiments and numerical simulations. One of the correlations in NFPA 92 has its roots back to Law's [34] interpretation of small-scale experimental data obtained by Morgan and Marshall [35]. This correlation is presented as:

$$\dot{m} = 0.36\left(\dot{Q}\dot{W}^2\right)^{1/3}(z_b + 0.25H) \qquad (51.30)$$

Lougheed et al. found that their large scale data was well described by this correlation for clear heights (z) in excess of 15 m. For lower heights, Lougheed et al. suggest the following correlation:

$$\dot{m} = 0.59\dot{Q}^{1/3}W^{1/5}(z_b + 0.17\dot{W}^{7/15}H + 10.35W^{7/15} - 15) \qquad (51.31)$$

The correlations presented in Equations 51.30 and 51.31, as well as others presented by numerous previous researchers, apply to balcony spill plumes of a specific configuration. The configuration considered is depicted in Fig. 51.9. As illustrated in the figure, the fire is located in a communicating space and the smoke flows under a soffit out from the room of fire origin, then under a short horizontal obstruction, i.e., balcony. The balcony is oriented perpendicular to the opening from the room. Any variations from

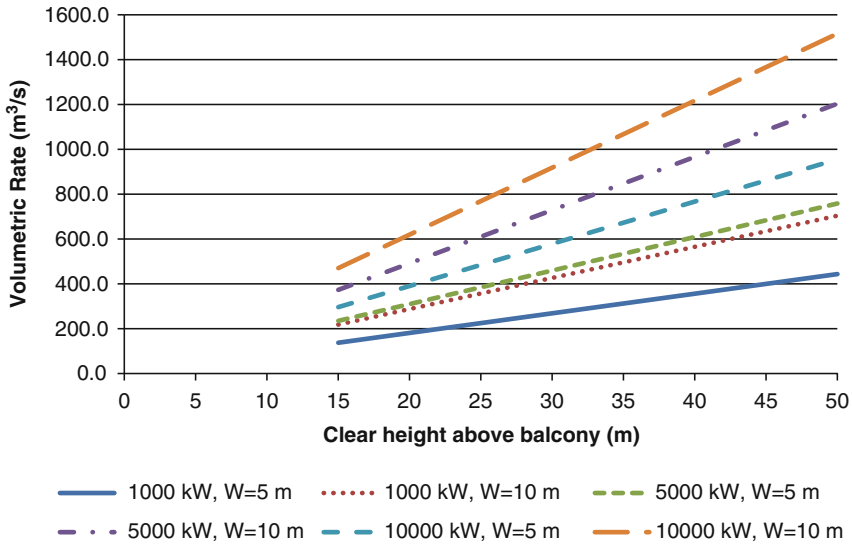

Fig. 51.9 Approximation of a balcony spill plume

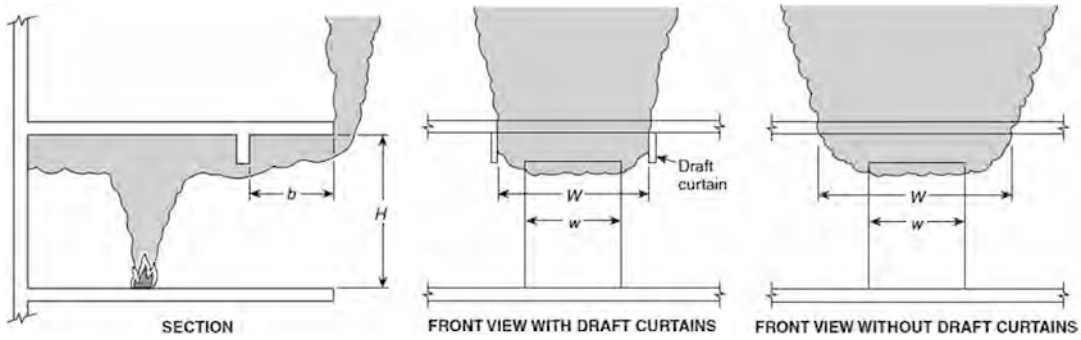

Fig. 51.10 Smoke production rate predictions for balcony spill plumes (H = 3 m)

this specific configuration have not been investigated and thus the balcony spill plume correlations presented as Equations 51.30 and 51.31 should not be applied for those situations. Instead, the application of CFD codes or small-scale models should be applied to assess those situations.

Predictions of the smoke production rate using Equation 51.30 for the balcony spill plume are included in Fig. 51.10. The calculations represented in the figure consider a 3-m height to the underside of the balcony.

A comparison of the smoke production rate for axisymmetric and balcony spill plumes is provided in Fig. 51.11. The results from both Equations 51.30 and 51.31 are depicted in Fig. 51.11 and are the reason for the points of inflection at a clear height of 15 m. The heat release rate for both fires is a steady state 5000 kW, and H is 3 m for the balcony spill plume. For short heights, the smoke production

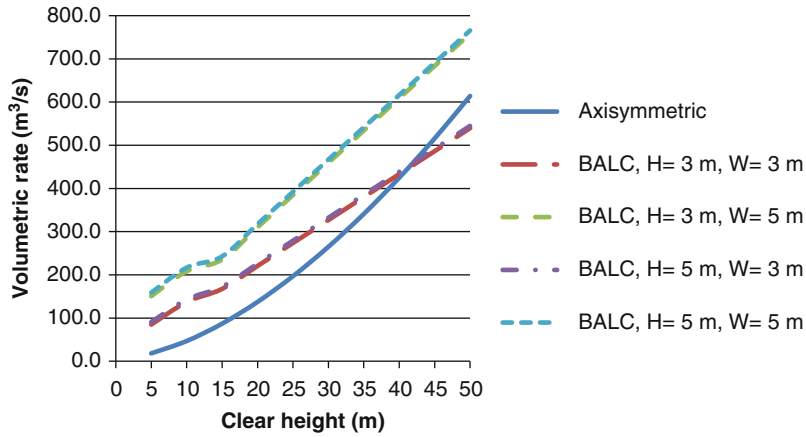

Fig. 51.11 Comparison of smoke production rate for axisymmetric and balcony spill plumes

rate for the balcony spill plume is appreciably greater than that for the axisymmetric plume. However, with increasing height, the smoke production rates from the two plumes become comparable. Eventually, the two curves intersect, suggesting that, at some height, the balcony spill plume behaves in the same manner (i.e., produces the same amount of smoke) as an axisymmetric plume. The point of intersection can be determined by setting the mass flow in Equation 51.27 equal to that in Equation 51.30.

The width of the plume, W, can be estimated by considering the presence of any physical vertical barriers attached to the balcony. The barriers act to restrict dispersion of the horizontal flow of smoke under the balcony. However, in the absence of any barriers, an equivalent width can be defined, based on results from visual observations of the width of the balcony spill plume at the balcony edge from the set of small-scale experiments by Morgan and Marshall [35]. The definition of an *equivalent confined plume width* is the width that entrains the same amount of air as an unconfined balcony spill plume. The equivalent width is evaluated using the following expression

$$L = w + b \tag{51.32}$$

Properties of Smoke Layer

Properties of the smoke layer are of interest both during the filling period of the fire and during the vented period. During the filling period, determination of the smoke layer properties is important to assess the level of hazard prior to actuation of a mechanical smoke control system. During the vented period, smoke layer properties are of interest to assess the level of hazard associated with those cases where occupants are exposed to smoke (i.e., the highest walking level is submerged in the smoke layer). The smoke layer properties of interest include temperature, light obscuration, and gas species concentration.

Temperature Rise in Smoke Layer The temperature of the smoke layer can be determined based on an energy balance for the volume of the smoke layer. Energy is supplied to the layer by the fire. Energy may be lost from the layer to the enclosure (walls, ceiling) of the space. During the filling period, the resulting expression is [1].

$$T = T_o \exp\left(\frac{(1-\chi_l)Q}{Q_o}\right) \tag{51.33}$$

Estimates for χ_l (heat loss fraction from the smoke to enclosure) vary appreciably. Some of the design guides suggest assuming that the smoke layer is adiabatic (i.e., setting $\chi_l = 0$), in order to be conservative [1]. Walton suggested values for χ_l between 0.6 and 0.9 for relatively small spaces of near cubic shape [36]. In many of the large spaces with tall ceiling heights, the temperature rise anticipated for the smoke layer is relatively modest such that convection and radiation heat transfer to an

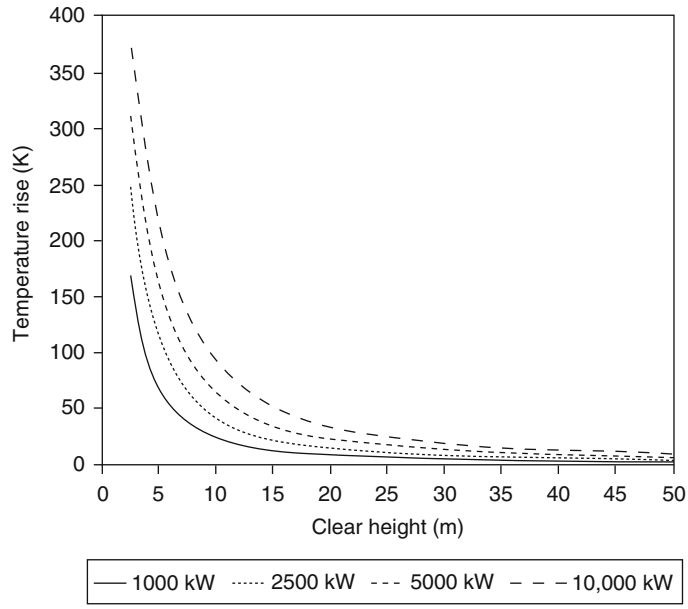

Fig. 51.12 Temperature rise of smoke layer for axisymmetric plumes

enclosure will also be modest. Consequently, in such applications, the adiabatic assumption will provide reasonable predictions of the temperature rise. However, in low ceiling spaces (under approximately 10 m) the temperature may be significantly overestimated by applying the adiabatic assumption.

Similarly, the equilibrium smoke layer temperature during venting can be approximated by applying an energy balance to the smoke layer. In this case, energy is also lost from the layer due to smoke being exhausted from the atrium. Equation 51.34 can be used to determine the temperature rise of the smoke layer under adiabatic conditions.

$$\Delta T = \frac{(1-\chi_l)\dot{Q}_c}{c_p \dot{m}} \tag{51.34}$$

If the adiabatic assumption is applied, the smoke layer temperature will be overestimated, providing a conservative estimate of the hazard. In reality, some heat is lost from the upper smoke layer to the surrounding walls and ceiling. However, no elementary method is available to estimate the overall proportion of heat that is lost to the surroundings [37, 38]. Some zone and field computer fire models account for heat losses to the boundary, thereby avoiding the need to specify the heat loss fraction [19, 39]. The adiabatic smoke layer temperature for a range of fire sizes is presented in Fig. 51.12.

The degree of overestimation can be assessed by comparing the estimated smoke layer temperature with the plume centerline temperature. For thermodynamic reasons, the smoke layer temperature cannot exceed the plume centerline temperature. The plume centerline temperature, T_c, can be evaluated using Equation 51.35 [40]

$$T_c = 0.08 T_o \dot{Q}_c^{2/3} z^{-5/3} + T_o \tag{51.35}$$

The volumetric venting rate for other heat release rates or temperature rises may be determined using Equation 51.36 considering that the specific heat is virtually constant for the expected temperature range of interest

$$\frac{\dot{Q}_{c_1}}{\dot{Q}_{c_2}} = \frac{V_1}{V_2}\frac{\Delta T_{\mathrm{ad}_1}}{T_{\mathrm{ad}_2}}\frac{T_2}{T_1} \tag{51.36}$$

As can be observed from Equation 51.36, doubling the volumetric venting rate for the same size fire reduces the temperature rise by approximately 50 % (the temperature rise is not precisely halved, since the absolute temperature of the smoke layer in both instances is not exactly the same).

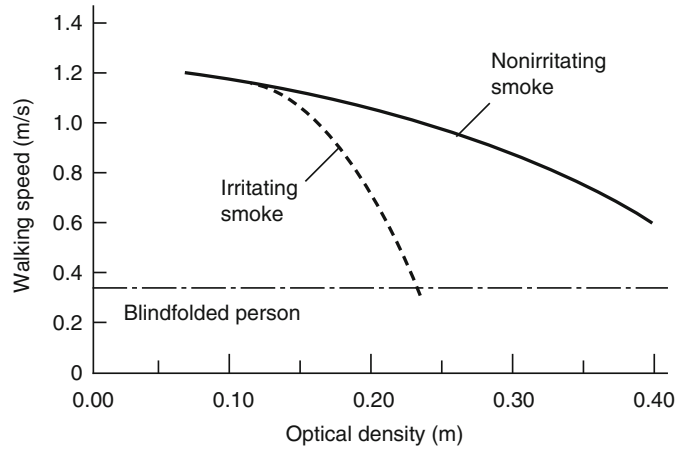

Fig. 51.13 Relationship between visibility through smoke and walking speed

Light Obscuration The visibility distance through smoke can be related to the optical density per unit pathlength via empirical correlations [41, 42]. The experimental basis for the correlations consists of tests with humans viewing objects through smoke. However, the participants were not directly exposed to the irritating effects of smoke. Consequently, the reported correlations are likely to overestimate the visibility distance.

In addition to the light obscuration quality of the smoke, the visibility of an object is dependent on the light source for the object being viewed as well as ambient lighting conditions [42, 43].

The optical density of the smoke layer can be determined considering that all of the particulates generated by the fire are transported to the layer via the plume and accumulate in the layer. Such an approach neglects any deposition of soot on enclosure surfaces, thereby overestimating the optical densities. The expressions for the smoke filling and vented periods are provided as Equations 51.37 and 51.38 [16].

$$\text{Smoke filling}: \quad D = \frac{D_m Q}{\chi_a H_c A (H - z)} \tag{51.37}$$

$$\text{Vented}: \quad D = \frac{D_m \dot{Q}}{\chi_c \Delta H_c \dot{m}/\rho} \tag{51.38}$$

The mass optical density is dependent on the fuel, burning mode, ventilation conditions, and operation of sprinklers. The mass optical density can vary by orders of magnitude for different ventilation conditions.

Although a reduction in visibility is not directly life-threatening, it does reduce the walking speed of individuals, thereby increasing the exposure time to toxic gases and elevated temperatures. In addition, the reduction in visibility may lead to an increased susceptibility to occupants tripping or falling. The relationship between visibility and movement speed is indicated in Fig. 51.13.

Carbon Monoxide Concentration The concentration of gas species contained in the smoke layer can be determined considering that all of the mass that is supplied to the layer via the plume accumulates in the layer. No absorption by the enclosure is assumed. The resulting expressions for the smoke filling and vented periods are [16].

$$\text{Smoke filling}: \quad \Upsilon_i = \frac{f_i Q}{\rho_o \chi_a H_c A (H - z)} \tag{51.39}$$

$$\text{Vented}: \quad \Upsilon_i = \frac{f_i Q}{\dot{m} \chi_a H_c} \tag{51.40}$$

In order to express the gas species concentration in units of ppm, Equation 51.41 needs to be applied

$$ppm_i = \frac{MW_{air}}{MW_i}\gamma_i \times 10^6 \qquad (51.41)$$

Input for evaluating the gas species concentration includes the yield fraction and heat of combustion, both of which are fuel dependent parameters. The yield fraction is dependent on the burning mode and oxygen concentration. Most of the information tabulated on the yield fraction, such as that by Khan (see Chap. 36), assumes well-ventilated, flaming combustion. Most of the fires of interest in large spaces will involve flaming combustion and are likely to be well ventilated. However, fires in small, connected spaces may become underventilated. Caution needs to be exercised in properly identifying ventilation conditions when predicting these parameters because the yield fraction can vary by orders of magnitude for different ventilation conditions. Also, the yield fractions noted by Tewarson are relevant only to cases where sprinklers are not operating [44].

Example 7 Estimate the steady-state smoke layer properties (temperature, visibility to an internally illuminated exit sign, and CO concentration) during the vented period, given the following situation:

1. The smoke layer interface is maintained 35 m above floor level.
2. The rate of heat release of the flaming fire is a steady state 5000 kW.
3. The fuel is comprised principally of polyurethane foam.

SOLUTION *Smoke Layer Temperature*
Equation 51.34 can be applied to determine the adiabatic smoke layer temperature rise. In Example 5, a mass rate of smoke production of 410 kg/s was determined. Thus, assuming an adiabatic smoke layer, a convective heat release rate fraction of 0.7 and specific heat of air of 1.0 kJ/kg·K, the temperature rise is 8.5 °C.

Visibility Visibility during the vented period is estimated using Equation 51.38. Fuel-related parameters are obtained in Chaps. 36, 24.

$$D_m = 260\ \mathrm{m^2/kg}$$
$$H_c = 12{,}400\ \mathrm{kJ/kg}$$

Considering smoke layer density, ρ, at the temperature of the smoke layer to be 1.17 kg/m^3, the optical density is 0.32 m^{-1} and the associated visibility is 8.5 m.

CO Concentration CO concentration for the vented period is estimated using Equations 51.40 and 51.41, with the fuel-related properties again evaluated from, Appendix C.

f_{CO} for polyurethane is ~ $0.030 \mathrm{kg_{co}/kg_{fuel}}$

The resulting CO concentration in the smoke layer is 31 ppm.

Comparison of Mechanical Exhaust and Natural Venting Designs

Design Aspects of Mechanical Venting Systems

Most smoke control systems for covered malls and atria in the United States use mechanical venting systems. Mechanical venting systems need to be designed to exhaust the amount of smoke needed to satisfy design objectives. The volumetric flow of smoke needs to be adjusted for temperature, using the methods discussed previously in this chapter.

Mechanical exhaust systems are relatively immune to environmental effects because the energy associated with the fan is able to provide a sufficient force for smoke movement and, thus, is not relying as much on the buoyancy of the smoke or stack effect. Protection from wind effects can be accommodated by hardware.

Response time is a principal limitation for mechanical exhaust systems. The response time is the sum of the time for detection and the time for the system to reach capacity (which may be up to a minute). This combined time may be longer than the time for the smoke layer to reach the critical height established by design goals. Also, because the capacity of a mechanical venting system is sized considering a particular

size of design fire (see Equations 51.26, 51.27, 51.30 and 51.31), if an actual fire has a greater heat release rate than considered in the design, the capacity of the mechanical exhaust will not be sufficient.

In addition, mechanical exhaust systems are susceptible to plugholing, a situation in which a hole is created in the smoke layer below the exhaust inlet by a high-capacity exhaust system. This results in a reduction in efficiency of the exhaust system because air from beneath the smoke layer is being extracted, thereby the desired quantity of smoke is not being extracted, causing the smoke layer to deepen. Plugholing is addressed later in this chapter.

The limitations of mechanical venting systems can be overcome in some cases by providing detection devices that minimize the time required for detection and by using several small capacity exhaust fans to avoid plugholing. However, despite these measures, it is still possible that design goals will not be able to be achieved by mechanical venting designs. Thus, the feasibility of such goals may need to be evaluated. Alternative smoke management approaches may be sought, for example, providing physical barriers at upper levels to reduce the required clear height or considering opposed airflow at openings above the design smoke layer interface position.

Design Aspects of Natural Venting Systems

Natural venting removes smoke by taking advantage of the buoyancy of the smoke. In the United States, natural venting systems are primarily found only in facilities such as industrial or warehouse structures. Outside of the United States, natural venting is often utilized in many applications.

The key advantages of natural venting systems are the self-correcting aspect of the vents in case the design fire is inappropriately defined and the simplicity of the operation of natural vents. These advantages will be described as part of the continuing discussion in this section.

The engineering principles that apply to vent operation addressed in this section consider the scenarios depicted in Fig. 51.14. Because smoke filling along the underside of the ceiling in a curtained area is similar to that in a compartment, additional information on compartment fire scenarios is presented in Chap. 33. If the draft curtains are deep enough, they can be thought of as simulating the walls of a single compartment.

The description of engineering principles of natural vents will be provided from the perspective of a two-layer zone model. The overall building compartment is assumed to have near-floor inlet vents that are large enough to maintain the area below the smoke layer at outside-ambient conditions. The upper smoke-layer thickness will change with time, but at any instant it is assumed to be uniform in space, with absolute temperature, T, and density, ρ.

Mass and energy are transferred continuously to and from the upper and lower layers. Conservation of energy and mass along with the Ideal Gas Law is applied to the layers, which leads to equations that require estimates of components of heat transfer, enthalpy flow, and mass flow to the layers. Qualitative and some key quantitative features of these phenomena are described and presented below. The reader is referred to Chap. 15, for a general discussion on the topic of flow through vents. Considering a vent in a wall or ceiling, flow is driven through such a vent mainly by cross-vent hydrostatic pressure differences from the high- to the low-pressure side of the vent. The traditional means of calculating vent-flow rates is by using an orifice-type flow calculation.

Assuming relatively quiescent conditions in the areas on both sides of the vent, the pressure in each space can be described as the hydrostatic pressure. The mass flow through a vent is derived from Bernoulli's equation, where the buoyancy pressure is related to the dynamic pressure at the vent:

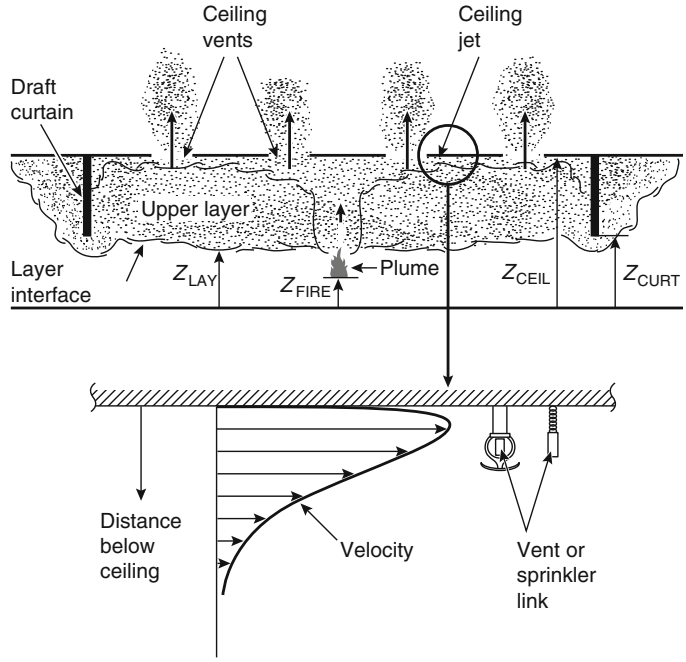

Fig. 51.14 Fire in a building space with draft curtains and ceiling vents

$$\frac{1}{2}\rho_o \mu^2 = \Delta\rho g d \tag{51.42}$$

where
ρ = Density of smoke (kg/m^3)
ρ_o = Density of ambient air (kg/m^3)
$\Delta\rho = \rho_o - \rho$ (kg/m^3)

Relating the mass flow through the vent to the velocity of the gases

$$\dot{m} = \rho A_v u \tag{51.43}$$

where
$\dot{m}$ = Mass flow rate through vent (kg/s)
A_v = Flow area of vent (m^2)

Replacing the densities with temperatures using the ideal gas law:

$$\dot{m} = \left(2\rho_o^2 g\right)^{1/2} \left(\frac{T_o \Delta T}{T}\right)^{1/2} A_v d^{1/2} \tag{51.44}$$

As indicated in Equations 51.42–51.44, the capacity of natural vents is related to the pressure difference caused by the buoyancy of the smoke layer. As such, the flow rate of smoke through the vent increases with increasing smoke-layer temperature and depth.

$$\dot{m} = \left(2\rho_o^2 g\right)^{1/2} \left(\frac{T_o \Delta T}{T^2}\right)^{1/2} \frac{A_v d^{1/2}}{\sqrt{1 + \frac{C_{d,v}^2 A_v^2 T_o}{C_{d,i}^2 A_i^2 T_o}}} \tag{51.45}$$

For vents installed in sloping roofs, the design position of the smoke layer should be at least below the bottom of the vent. To ensure that only smoke is exhausted from that vent and not any air from below the layer, the smoke layer position should be at least 10 % of the vertical distance from the top of the vent (Fig. 51.15). Then the distances d and z (recall that clear height is imbedded in the consideration of $\dot{m}$) are measured from the center of the vent.

Makeup Air Supply The effect of the inlet area on the flow rate through the vent can be assessed by recognizing that the pressure drop across the inlets associated with the inflow of replacement air must be subtracted from the buoyancy pressure causing the gases to flow through the vents. The effect of inlet pressure may be included in Equation 51.45 by replacing A_v by an effective vent area $\left(A_v^*\right)$ where

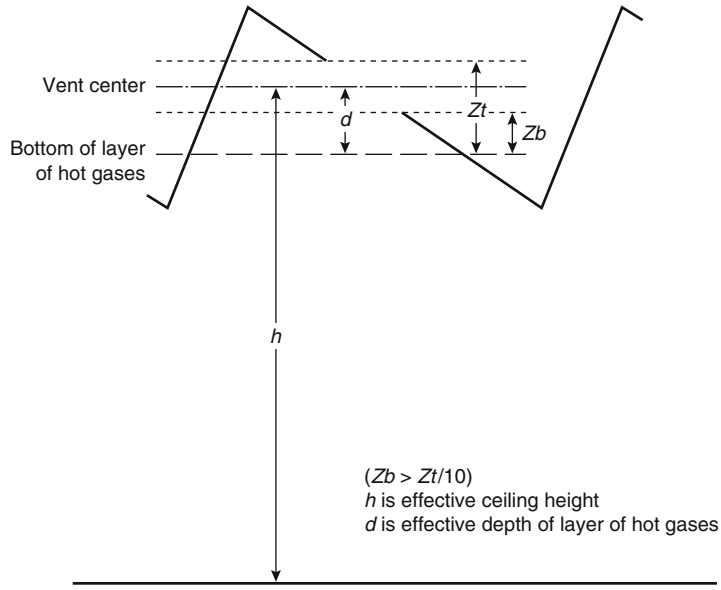

Fig. 51.15 Design position of gas layer versus vent

$$\frac{1}{A_v^{*2}} = \frac{1}{A_v^2} + \frac{1}{A_i^2}\left(\frac{T_o}{T}\right) \tag{51.46}$$

As such, the ratio of the actual vent area to the effective vent area, K, is given as

$$K = \frac{A_v}{A_v^*} = \left[1 + \left(\frac{A_v}{A_i}\right)^2 \frac{T}{T_o}\right]^{1/2} \tag{51.47}$$

The effect of vent ratio (ratio of outlet to inlet areas) on the effectiveness of natural venting is presented in Fig. 51.16 with a design fire of 2.5 MW and a ceiling height of 15 m. As indicated in the figure, with a vent ratio of 0 (having infinite inlet area), the clear height is slightly greater than when the outlet to inlet areas are equal. Thus, as with mechanical systems, the inlet area is an important consideration.

One of the principal advantages of natural venting systems is the relative insensitivity of the equilibrium smoke-layer position with the fire size, as indicated in Fig. 51.15. The graphs in Fig. 51.17 indicate that for two different ceiling heights (15 and 30 m), the equilibrium smoke-layer temperature is virtually identical for the two significantly different fire sizes. This similarity is due to the bigger fire size producing a smoke layer with a greater temperature. The hotter smoke will be more buoyant, thereby increasing the buoyancy force at the vent leading to an increase in the mass flow rate through the vent to reduce the amount of smoke accumulating under the ceiling.

The ability of a vent to perform similarly for two different fire sizes is a significant benefit of natural vents. Unlike mechanical exhaust, for natural vents if an error is made such that an actual fire is greater than the defined "design fire," the natural vents should still able to provide near-satisfactory performance.

Limitations The limitations of natural venting systems are related to the forces affecting smoke movement: principally a lack of buoyancy and wind effects. The smoke must be buoyant relative to the ambient environment in order for natural venting systems to be effective. Smoke may lose its buoyancy either due to cooling from sprinkler operation or dilution from entrained, cool air. Because the mass flow is strongly dependent on the difference in the smoke-layer temperature and outdoor temperature, if the smoke-layer temperature rise is only slightly different than the ambient temperature, then the flow from a vent will also be modest. As such, in tall spaces with relatively small fire sizes, the

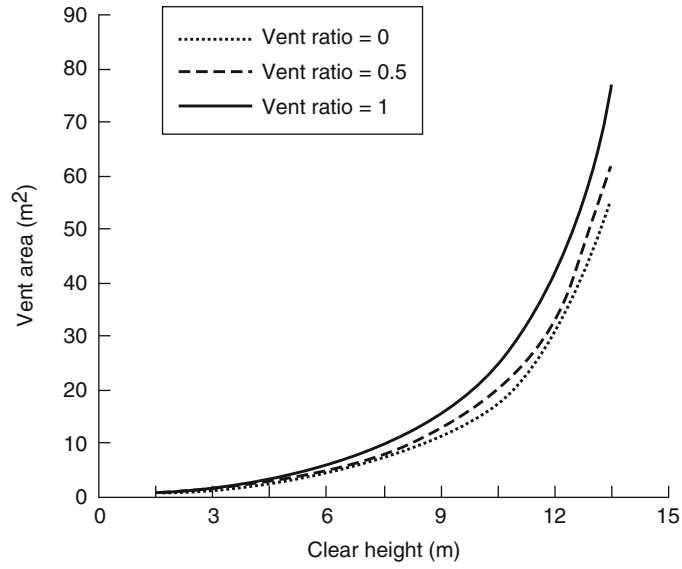

Fig. 51.16 Effect of vent ratio on natural venting

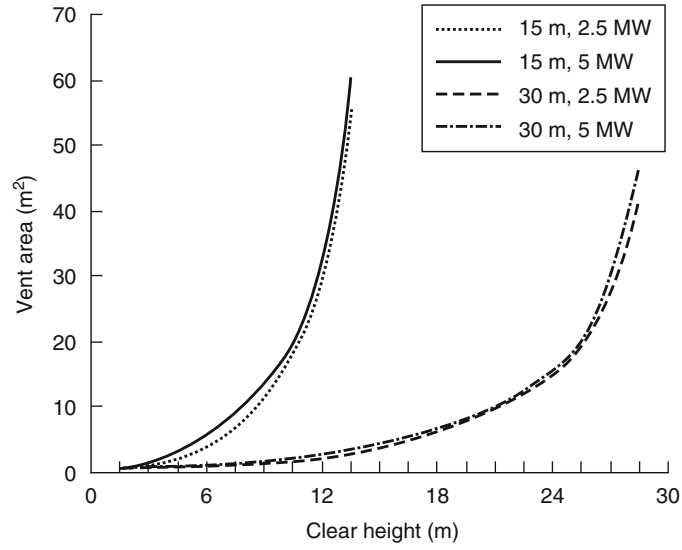

Fig. 51.17 Effect of vent ratio on natural venting for two ceiling heights (15, 30 m) and fire sizes (2.5 MW, 5 MW)

modest capacity of natural vents may constrain the ability to achieve design objectives, necessitating that mechanical ventilation be used.

To consider the effect of outside wind conditions, pressures on the outside of the building in the vicinity of the vent need to be assessed. The pressure on the building depends on the wind speed at the elevation of the vent, wind direction relative to the outside building geometry, and proximity and geometry of neighboring buildings. Wind effects on buildings are addressed in Klote et al. [2].

If the building vents are open and if vent areas are relatively small compared to the building surface area, then pressures near the vent openings will be substantially unchanged from the above-mentioned, closed-vent pressure distribution, except near any local through-vent flows that may develop. Also, although the

exterior pressures generally vary from vent to vent, they will be relatively uniform for any particular vent. Under these conditions, a determination of flow rates into and/or out of vents and through the interior of the building is based on an interior building flow analysis, with pressure-specified boundary conditions at the open vents.

A Single, Open Inlet Vent or Multiple Openings at the Same Pressure If there is only one open inlet vent on the upwind side of the building that experiences a relatively high pressure differential above the local hydrostatic pressure or if there are several open vents, all at locations on the outside surface of the building where pressures are substantially identical, then, the wind will have no effect on the inflow or outflow through the vents. Thus, if the air inside the building is uniformly at the outside air temperature and if there is no mechanical ventilation, then the effect of the wind will be simply to bring the interior hydrostatic pressure at the location of the vent(s) to the aerodynamic-flow-specified value; the interior of the building will be "pressurized" as a result of the open vent(s), but there will be no wind-induced interior flows. If there is a fire in the room with the open vent (e.g., the vent is a broken window), then, in the usual way, there will be fresh air inflow into the room toward the bottom of the vent and buoyant smoke outflow toward the top of the vent, all this taking place at an aerodynamic-flow-specified, elevated hydrostatic pressure within the room.

If the open vent is in a side of the building with a negative wind coefficient (e.g., facing downwind or on roofs near the upwind side), the pressure at the vent will be relatively low, and the local hydrostatic pressure will be *reduced* by an amount only on the order of $\rho_o u^2/2$. Again, no wind-induced flow at the vent is expected.

Two Inlet Vents, One on the Upwind Side and One on the Downwind Side of the Building If there are two inlet vents in the walls of the building, one upwind and one downwind (ignoring heating and mechanical ventilation), then there *will* be wind-induced flow through the vents and within the building. Inlet air will be provided at the high-pressure upwind vent and outlet air at the low-pressure downwind vent, with levels of through-vent flows and of interior hydrostatic pressures determined by an appropriate analysis that accounts for conservation of momentum (i.e., Bernoulli's equation) and mass at the exterior vents and at room-to-room vents within the interior of the building. The changes in hydrostatic pressures within the rooms of the building, over and above the hydrostatic pressures that would be present in a quiescent environment, would be somewhere between the wind-induced pressures at the locations of the high-pressure vent and the low-pressure vent.

Wind-Modified Pressures at Roof Surfaces and Wind-Modified Action of Ceiling Vents Roof surfaces of flat-roofed buildings tend to have negative, wind-induced pressure coefficients, unless the buildings are very long in a direction parallel with the wind direction. Sloping roofs may have pressure coefficients that can be positive or negative, depending on wind direction. Therefore, if the interior, wind-induced hydrostatic pressures are greater than those associated with a quiescent environment (e.g., the result of open vents in the upwind side of the building), then the flow of smoke through ceiling vents can be enhanced significantly by virtue of increased, favorable, cross-vent pressures. However, for reduced interior pressures (e.g., as a result of open vents on the downwind side of the building), the effect of wind conditions can substantially disrupt the desired smoke-removing action of ceiling vents, even reducing the *direction* of the cross-vent pressures and, as a result, the direction of the flow through the vents (i.e., making the flow travel from the outside to the inside).

Thermal Activation of Vents

Convective heating and thermal response of near-ceiling-deployed fusible links or other near-ceiling thermal sensor devices (including thermoplastic vent covers designed to soften

and "drop out" at specified actuation design temperatures) are determined from the local time-dependent distributions of ceiling jet velocity and temperature. These distributions will depend on vertical distance below the ceiling and radial distance from the fire-plume axis. Once the operating temperature of the thermal element is reached, the device or devices operated by the element will be actuated. Characteristics of ceiling jets are described in Chap. 14.

The mathematical fire model LAVENT (fusible-*L*ink-*A*ctuated *VENT*s) [22–24] was developed and is available to simulate most of the phenomena described above. The LAVENT model can be used to simulate on a time-dependent basis and to study parametrically a wide range of scenarios with natural vents. Full documentation for LAVENT, including its theoretical basis [22], a user guide for the computer code [23], and sample problems using the code are included in Annexes B, C, and D of NFPA 204 [45]. In its current form, LAVENT does not account for wind effects, the reduced effectiveness of vents as a result of limited-area inlet vents, or the presence of mechanical systems [22]. Input data on the thermal response characteristics of the link will be needed for such an analysis. The use of LAVENT has not been validated for estimating the response of "drop out" vents.

Sprinklers and Vents

Vents and sprinklers provide different fire safety benefits. The level of fire safety in a facility would be enhanced if both sets of benefits could be achieved systematically. However, simply providing the two technologies following design rules independent of each other will not necessarily lead to a combination of their respective benefits. Potential problems may occur as a result of the interaction of the two technologies (i.e., operation of the smoke and heat vents can modify sprinkler performance and the operation of the sprinklers can modify smoke and heat vent performance). As an example of the latter, consider the case in which water spray from a sprinkler system cools the smoke, thereby reducing the buoyancy of the smoke. The reduced buoyancy reduces the mass flow rate through a vent, thereby resulting in a deeper smoke layer. However, the sprinkler discharge can also dramatically reduce the fire size resulting in a decreased production of smoke.

Numerous research projects have been conducted to address the interaction between vents and sprinklers (see Annex A of NFPA 204 and Beyler and Cooper [46] for a thorough review of the previous research). The previous projects have sought to demonstrate the level of impact that one system has on the other's performance, either by indicating that it is always significant, always insignificant, or significant only if a particular set of conditions is provided. Projects have also attempted to identify design changes necessary if both systems are present (i.e., perhaps larger vent sizes could be installed in sprinklered buildings to counteract the reduced mass flow of cooled smoke). To date, none of the previous projects have been able to provide the conclusive results that provide definitive information illustrating the degree of influence that one system has on the other for all situations.

Past Studies of Combined Vent/Sprinkler Systems A review of 34 papers evaluated the validity of generic claims and counterclaims on the benefits of combined vent/sprinkler systems [46]. A listing of these claims and counterclaims and a summary of conclusions on their validity follow.

Claims and Counterclaims [46] In the literature, claims that have been made in favor of vent/sprinkler systems can be reduced to the following three:

1. Smoke and heat vents limit the distribution of products of combustion in the facility whether deployed sprinklers are operative or inoperative.
2. Smoke and heat vents decrease the number of activated sprinklers.

3. Smoke and heat vents assist the fire department in identifying the location of the fire within the facility and in reducing the need for manual roof venting.

In the literature, claims that have been made *against* vent/sprinkler systems can be reduced to the following four:

1. Smoke and heat vents cause enhanced burning rates.
2. Smoke and heat vents delay sprinkler activation.
3. Smoke and heat vents increase the number of activated sprinklers.
4. Smoke and heat vent flow rates are insufficient to realize any benefit.

Validity of Claims for and Against Combined Vent/Sprinkler Systems After evaluating reports of studies of combined vent/sprinkler systems, Beyler and Cooper [46] came to the following conclusions:

- Venting does not have a negative effect on sprinkler performance.
- If a fire is directly beneath a vent, activation of the first sprinklers may be delayed slightly, but there is no evidence that this delay will have a significant impact on overall sprinkler performance.
- Venting does limit the spread of smoke by removing smoke from the building near the source of the fire (within the curtained compartment of fire origin), improving visibility for building occupants while evacuating and for fire fighters during fire control operations.
- By limiting the spread of smoke and heat, venting reduces smoke and heat damage to the building.
- In the event that sprinklers do not operate, venting remains a valuable aid in controlling the fire manually.
- In many fires, current vent design practices, for example, those of NFPA 204 [45], are likely to limit the number of vents operated to one and, in successful sprinkler operations, vents may not operate at all.
- Design practices should use methods that ensure early operation of vents; vent operation should be ganged so that the benefit of roof vents is fully realized.
- When deployed with vents and draft curtains, a sprinkler design needs to take full account of draft curtains as obstructions to ceiling jet flows and sprinkler discharge.
- Draft curtains should be placed in aisles rather than over storage.

Considerations for the Design of Combined Vent/Sprinkler Systems Taking Beyler and Cooper's conclusions into account and drawing on current knowledge of basic physical phenomena involved in vent/sprinkler interactions, the design of combined sprinkler/vent systems should seek to satisfy the following general criteria:

1. A successful vent design, whether deployed with or without sprinklers, is one that leads to the benefits of improved visibility and safety during a fire by limiting the descent of the upper smoke layer to a specified height (i.e., eye level of occupants and fire fighters).
2. When draft-curtain compartmentation is included in the vent design, a significant additional possible benefit results from the smoke being contained within the curtained compartment of fire origin by action of the venting.

Interaction of Sprinkler Spray and Smoke Layer The action of sprinkler sprays on a smoke layer includes a combination of evaporative cooling and dilution of the smoke. Dilution occurs due to entrainment of the relatively cool and uncontaminated lower-layer gases and the upper layer by the spray [47–59]. Provided the sprinkler spray–reduced smoke temperature and associated loss of buoyancy are not too great, the effect of evaporative cooling of the smoke, even if accompanied by moderate sprinkler spray–driven mixing, could be offset by additional vent capacity. However, even without significant evaporative cooling, sprinkler spray–driven mixing action can be so significant that it leads to a precipitous increase in the volume of smoke and thus a deeper smoke-layer. If and when the latter vigorous mixing occurs, then even impractically large increases in vent capacity are unlikely to lead to any significant

improvement. The latter phenomenon is commonly referred to as *smoke logging*. As such, a vent design that is developed to meet the above general criteria must be based on an analysis that accounts for and avoids the phenomena of smoke logging.

There is experimental evidence that smoke logging can be controlled by venting [60], and a preliminary analysis to explain the phenomenon has been provided [47, 48]. Thus, it has been reported that "preliminary tests in [a] . . . large-scale mall . . . showed that, under some conditions, [a] . . . smoke layer could be brought down by a manually operated sprinkler spray, [and that] smoke logging then occurred rapidly, with a high smoke density at low level. However, under some conditions, the smoke layer was not disturbed by a sprinkler spray" [48].

Computer Simulations of Sprinkler Spray–Driven Cooling, Mixing, and Smoke Logging A computer model could be applied to address the issue of sprinkler spray–driven cooling, mixing, and smoke logging. However, the past experimental studies have not led to an understanding of the complex phenomena of sprinkler spray cooling and sprinkler spray–driven smoke transport and mixing that causes the temperature reduction that could be used as a basis for such a model. What is known through anecdotal accounts of visual observations is that spray-driven mixing and transport of an initially stable and growing upper smoke layer can and often does lead to onset of smoke logging, whereby the mixing actions of sprinkler sprays are so vigorous as to effectively and continuously mix any newly generated smoke from the fire plume with the smoke already present in the smoke layer to fill the entire space.

Analytic fire-modeling has been employed to assess a generic interaction of a downward-directed sprinkler spray and a two-layer fire environment can be used to resolve the above issues [59]. The model simulated the action of the sprinkler spray, including the effects of evaporative cooling and the spray-driven mixing of the elevated-temperature, upper smoke layer and the relatively cool and uncontaminated lower layer. The analysis led to the identification of six possible modes of sprinkler/layer interaction [58, 59]. The mode that prevailed at any time during the development of a particular fire was found to depend mainly on the thickness and temperature of the upper smoke layer and on the momentum, spread angle, and characteristic droplet size of the sprinkler spray. In any particular fire scenario, the action of open vents and/or draft-curtain compartmentation could provide some control of the thickness and temperature of the layer and, therefore, of sprinkler/layer interactions that prevail.

Of the six above-referenced modes of sprinkler/vent interaction, four were found to be particularly favorable in the sense that they would *maximize* the success of a combined sprinkler/vent design. Thus, with proper vent design the favorable modes could lead to the desired control of the smoke-layer depth while minimizing smoke mixing to the lower layer to the point that any smoke there is only in a highly dilute state. Thus, for a given set of sprinkler spray characteristics, if the smoke layer is kept relatively thin and/or not too buoyant (i.e., its temperature is not too high), then the rates of both mass and enthalpy flow entrained into the upper-layer part of the sprinkler's "spray cone of influence" would be relatively insignificant compared to the corresponding rates associated with the fire-plume flow to the upper layer. In the early part of a typical fire scenario and immediately subsequent to one or more rapid-response sprinkler discharges, the condition of a relatively thin and not-too-high-temperature upper smoke layer should be prevalent. As a result, the combined action of cooling and momentum exchange in the spray cone would be strong enough to transport the entrained smoke through the layer interface and well into the depth of the lower layer to be mixed eventually, with negligible consequences, into the rest of the lower-layer gases.

In contrast to the above, there were two particularly *unfavorable* modes of sprinkler/vent interaction that would *minimize* the likely success of a combined sprinkler/vent design. These configurations could lead to relatively vigorous

mixing between the smoke layer and the lower layer, leading to a rapid growth of the upper smoke layer and possibly to smoke logging.

Resolving the Problem of Sprinkler Skipping and Vent Skipping In terms of achieving vent/sprinkler design objectives, it is important to identify a possible means of resolving problems associated with the phenomena known as *sprinkler skipping* and *vent skipping*.

If ceiling jet–convected water droplets strike a sprinkler link or bulb, then, because of effects of evaporative cooling, there will be a significant reduction of its rate of heating, which can lead to a significant delay in sprinkler discharge. It is the resulting, unpredictable, and deleterious delay in sprinkler discharge that is referred to as *sprinkler skipping*.

Although research has been conducted to characterize the spray from sprinklers, a general description of all aspects of the spray is beyond the current state of knowledge. Such a description would be needed to provide a reliable model that can be used to predict the phenomenon.

Accounting for Sprinkler Skipping and Vent Skipping in Design In the design of sprinklers without vents, the effects of sprinkler skipping on the ability of a sprinkler system to control a fire are taken into account by the empirically based design standard, NFPA 204. In contrast, when vents and sprinklers are used *together,* the random and unpredictable effects of vent skipping are not accounted for in the design of automatic vent systems as outlined in NFPA 204.

In terms of combined vent/draft-curtain designs, and as an alternative to traditional automatic, fusible-link-actuated vents, which could involve the problem of vent skipping, a more controllable and reliable means of ensuring timely and effective vent action is available. One generic possibility would involve *ganging,* that is, opening together all or most vent units in the compartment of fire origin [61]. A ganging strategy that could be well integrated into a reliable, consensus sprinkler/vent design is one in which all vents of the fire compartment are ganged to open together immediately following first sprinkler discharge.

A Consensus Approach to the Design of Combined Sprinkler/Vent Systems

Using Mathematical Fire Models to Achieve Design Objectives The above discussion indicates that effective sprinkler/vent systems are feasible and that mathematical fire models with a proven capability for simulating sprinkler/smoke interactions can be used as the basis for a consensus approach to identify and establish effective sprinkler/vent system designs.

The capabilities of mathematical models to simulate sprinkler/smoke interactions have been reviewed [62, 63]. The models considered were those that are complete (i.e., they can simulate both isolated sprinkler/smoke interactions and full fire scenarios, where the latter would be used to establish the success of sprinkler/vent designs). Both zone-type and field model–type simulation approaches were found to be applicable for addressing the problem. In the usual way, the two approaches are complementary in the sense that the zone model approach is more applicable and appropriate for parametric studies and as a practical design tool and the field model approach is more applicable for simulating and studying the details of specific scenarios, for example, the discharge sequence of sprinklers and the effectiveness of a vent design where draft curtains are almost directly above the fire.

A sprinkler/vent design approach that uses zone-type fire model simulations might involve application of an advanced version of LAVENT that would include the sprinkler/smoke-interaction simulation model [59] discussed earlier. A successful preliminary implementation of this approach, with a revised prototype model called LAVENTS (fusible *L*ink-*A*ctuated *VENT*s and *S*prinklers), has already been presented [64]. Applications of the LES (*L*arge *E*ddy *S*imulation) model [65–68], the JASMINE model [69, 70], and others [71, 72] have also been reported.

One of the difficulties in applying the above for design applications is the limited availability of input data to describe the initial sprinkler spray from a wide range of sprinklers and the response characteristics of the vent.

A Set of Example Guidelines for Design of a Consensus Sprinkler/Vent System As a summary to the above discussion, the following example guidelines are provided for the design of a sprinkler/vent system.

1. Establish the sprinkler design in the traditional way; that is, develop design parameters using full-scale testing involving effective, rapid, sprinkler-activation strategies in the absence of vents (in this context, "rapid" means that the design problem involves an effectively unconfined ceiling where smoke-layer buildup is negligible and does not affect the timing or sequence of early sprinkler discharge).
2. Establish a vent design objective. In cases in which sprinkler action is expected to control the fire (i.e., the fire will not exceed a specified, maximum energy-release rate), the design objective for scenarios as shown in Fig. 51.13 might be for the vents to maintain indefinitely the smoke from spreading beyond the curtained compartment of fire origin (i.e., the smoke-layer interface does not descend below the bottom of the draft curtains). If the latter design objective is too ambitious or in cases in which sprinkler action is expected only to slow but not to stop the growth of the fire, then the design objective would be for the vents to maintain the smoke from spreading beyond the curtained compartment of fire origin for a specified time interval (e.g., the time expected for the fire department to respond and initiate an attack on the fire).
3. Adopt a practical/achievable strategy of early opening of all vents in the compartment of fire origin, e.g., ganged operation of all vents in the curtained compartment of fire origin based on and subsequent to first sprinkler activation.
4. Using a fire model with a proven capability of simulating the time-dependent interaction of sprinklers, vents, and draft curtains, develop a vent design that meets the established design objectives.

Special Conditions

There are some aspects of smoke control system design that involve special attention. These aspects, which affect actuation of active smoke control systems and the efficiency of exhaust fans, are the following:

- Intermediate stratification
- Confined flow
- Plugholing
- Makeup air supply

Intermediate Stratification

The upward movement of smoke in the plume is dependent on the smoke being buoyant relative to the surroundings. Delays in activation may be experienced where ceiling-mounted initiating devices are present if the air near the ceiling is warmer than the rising smoke [2, 73]. Dillon [74] reported measurements of the difference in ambient temperature from floor to ceiling to be on the order of 50 °C in some atria with glazed ceilings. A prefire, warm air layer may be created due to a solar load where the ceiling contains glazing materials. In such cases, the smoke will stratify below this warm air layer and not reach the ceiling. Early after ignition, the maximum height to which the smoke plume will rise depends on the convective heat release rate and the ambient temperature variation in the open space.

Algebraic correlations may be applied to address two situations (Fig. 51.18):

1. The temperature of the ambient air is assumed constant up to a height above which there is discrete increase in temperature associated with a layer of warm air. This situation may occur if the upper portion of a mall, atrium, or other large space is unoccupied so that the air in that portion is left unconditioned.
2. The ambient interior air within the large space has a constant temperature gradient

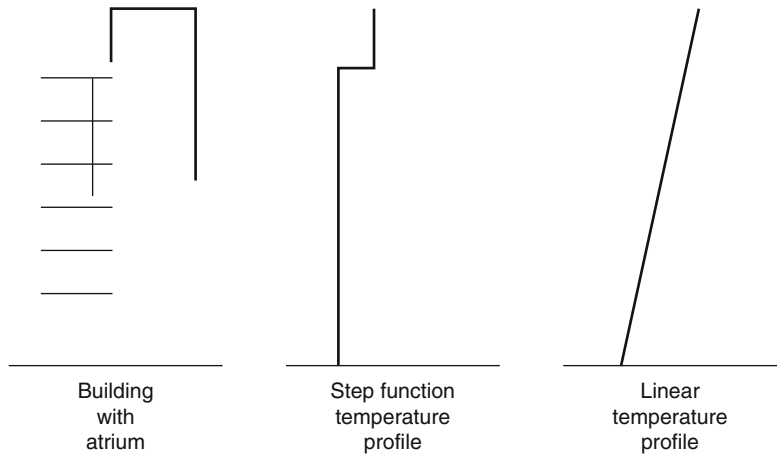

Fig. 51.18 Pre-fire temperature profiles

(temperature change per unit height) from floor level to the ceiling. This case is less likely than the first.

In the first case, where the interior air has a discrete temperature change at some elevation above floor level, then the potential for stratification can be assessed by determining the temperature of the plume at the height associated with the lower edge of the warm air layer. Where the plume centerline temperature is equal to the ambient temperature, the plume is no longer buoyant, loses its ability to rise, and stratifies at that height. One correlation for the plume centerline temperature was presented previously as Equation 51.35.

In the particular case where the ambient, pre-fire temperature increases uniformly along the entire height, the maximum plume rise can be determined from [19].

$$z_m = 3.79F^{1/4}G^{-3/8} \tag{51.48}$$

where

$$F = g\dot{Q}_c/(T_o\rho_o c_p)$$

$$G = -(g/\rho_o)d\rho_o/dz$$

Assuming standard conditions and that the smoke in the space behaves as an ideal gas, the expressions for F and G are

$$F = 0.0277\dot{Q}_c$$

$$G = 0.0335dT_o/dz$$

Because dT_o/dz is a constant, $\Delta T_o/H$ may be substituted for the derivative. Substituting the simplified expressions for F and G into Equation 51.48 yields [73].

$$z_m = 5.54\dot{Q}_c^{1/4}(\Delta T_o/H)^{-3/8} \tag{51.49}$$

By reformulating Equation 51.49 to solve for $\dot{Q}_c$, a minimum fire size can be determined that is just large enough to force the smoke to the ceiling of an atrium without prematurely stratifying due to the increasing ambient temperature.

$$\dot{Q}_c = 0.00118H^{5/2}\Delta T_o^{3/2} \tag{51.50}$$

The results of an analysis of intermediate stratification are presented in Fig. 51.19. In one case, a step function is assumed to provide a 30 °C change in temperature 15 m above the floor due to the upper portion of the atrium being unconditioned. For the other case, a temperature gradient of 1.5 °C/m is arbitrarily assumed in an atrium with a ceiling height of 20 m. Plume centerline temperatures from two size fires are graphed based on Equation 51.35. As indicated in the figure, for the case with the uniform gradient, smoke is expected to stratify

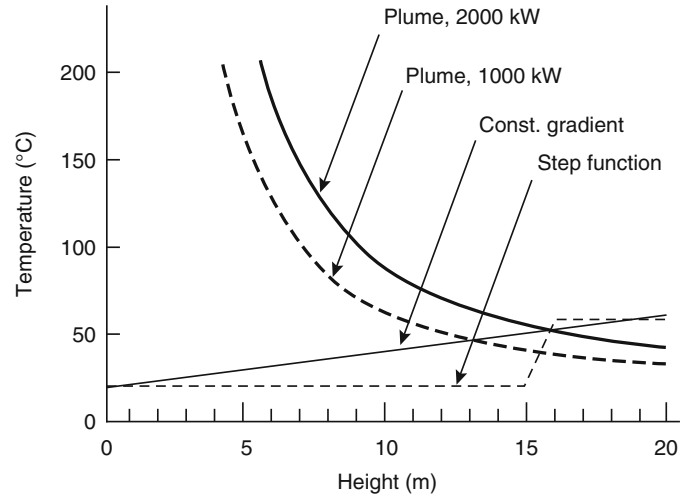

Fig. 51.19 Indoor air and plume temperature profiles with the potential for intermediate stratification

approximately 13 or 15 m above the floor, depending on the fire size. For the case involving the step function change in temperature, the smoke stratifies from both fire sizes at the height of the step change in temperature.

If the smoke is expected to stratify at an intermediate height below the ceiling, then a device other than ceiling-mounted detectors (such as projected beam detectors) needs to be considered to initiate the smoke control system. The beam detectors should be placed below the height of stratification to intercept the rising plume. In general, once the smoke control system operates, the warm air layer should be exhausted to permit the smoke to reach the ceiling.

Plume Width

As a plume rises it also widens as a result of the entrainment of additional mass into the plume. For tall, narrow spaces, the plume may fill the entire cross section of the atrium prior to reaching the ceiling. Above this position, air entrainment into the plume is greatly reduced due to the limited amount of air available. In such situations, initially the bottom of the smoke layer may be assumed to be located at this point of contact. Plume width is also important when determining the location of projected beam detectors intended to intercept the plume.

In order to determine the point of contact of the plume with the walls, the plume width must be expressed as a function of height. The width of the plume has been addressed theoretically and also experimentally.

Based on theory (see Chap. 13), the plume width is expected to be

$$d = 2.4\alpha z \tag{51.51}$$

where $\alpha \cong 0.15$

$$\text{Thus,} \quad d = 0.36z \tag{51.52}$$

Experimentally, the plume width is estimated by examining photographs [75] or the difference between the plume temperature and ambient temperature (i.e., temperature excess at various horizontal distances from the plume centerline) [30]. Using temperature measurements, the plume width is defined as the position where the temperature excess is one-half of the value at the centerline.

Handa and Sugawa [75] developed an empirical correlation of the width of the plume determined from photographs of the visual plume from wood crib fires

$$d = d_o z^{1/2} \tag{51.53}$$

Heskestad [76] noted that the visible plume diameter was greater than that determined from the temperature excess. Consequently, Heskestad

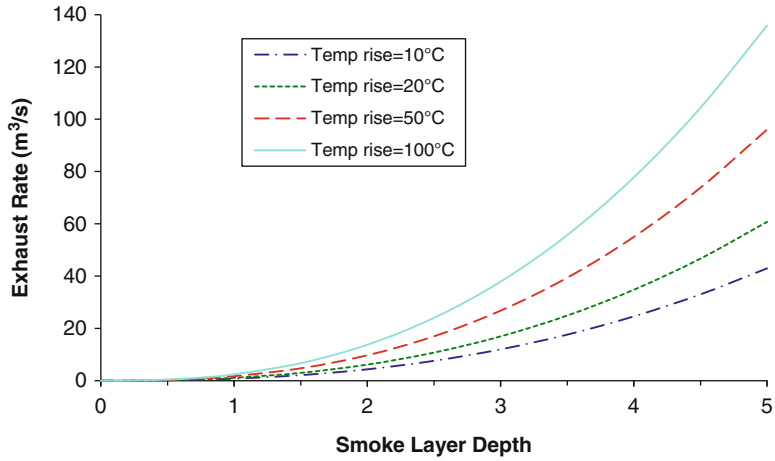

Fig. 51.20 Effect of smoke-layer depth and temperature rise on maximum exhaust capacity

estimated the visible plume diameter to be twice that determined by the excess temperature approach. Thus, the plume diameter is estimated as

$$d = 0.48\left(\frac{T_c}{T_o}\right)^{1/2} z \qquad (51.54)$$

As indicated in Equation 51.35, the plume centerline temperature decreases appreciably with increasing height. Thus, for tall spaces, the plume centerline temperature may be close to ambient. For example, at a height of 30 m with a fire size of 5000 kW and T_o of 293 K, T_c is 312 K. In this case $(T_c/T_o)^{1/2}$ in Equation 51.51 is only 1.03. Because of the rapid decline in T_c with increasing height, for engineering purposes $(T_c/T_o)^{1/2}$ can be approximated as being 1.0. Consequently, in many cases the total plume diameter may be approximated by considering the plume diameter to be approximately one-half of the height.

Considering the variety of analyses for plume width, the plume width is estimated to be 25–50 % of the height above the top of the fuel package, with the 36 % proportion from theory being near the middle of the range.

Plugholing

Plugholing occurs when the exhaust capacity at a single point is sufficiently large to draw air from the lower layer in addition to smoke. As such, less smoke is removed by the exhaust fans and a deeper layer results. Because a simple method to estimate the proportion of air drawn in from below the smoke layer by the fans is unavailable, an elementary method of estimating the smoke layer depth during plugholing is not available. As such, simple calculations can only be performed to assess the occurrence of plugholing, not the effect.

The original research on plugholing was done for natural vents. Recently, Lougheed and Hadjisophocleous demonstrated that the plugholing analysis for natural vents was also applicable to mechanical venting [77]. In order to avoid plugholing, the maximum exhaust capacity at an extract point is:

$$\dot{V}_{max} = 4.16\gamma d^{5/2}\left(\frac{\Delta T}{T_o}\right)^{1/2} \qquad (51.55)$$

Where γ is a factor relating to the location of the vent. If the vent is in the middle of the space, $\gamma = 1$ [1].

Results of applying Equation 51.56 are provided in Fig. 51.20 for a range of temperature rise values of the smoke. Where venting capacities greater than the maximum limit are needed to achieve smoke management objectives, multiple extract points need to be provided to avoid plugholing.

Assuming an axisymmetric plume, $\dot{m}$ can be replaced using Equation 51.20, and the smoke

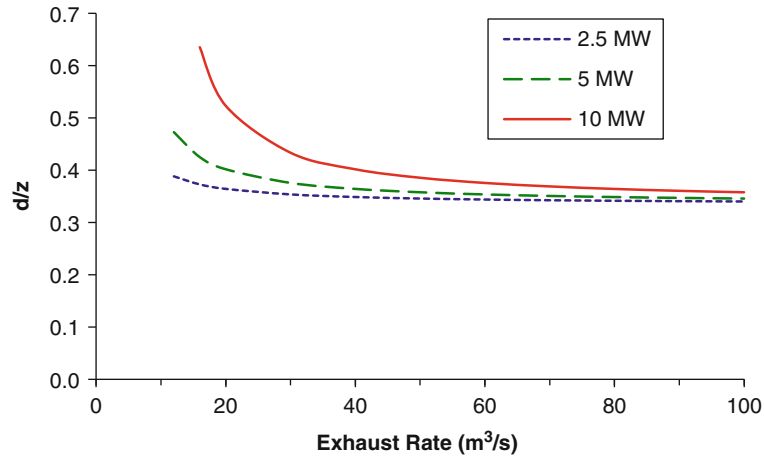

Fig. 51.21 Ratio of smoke-layer depth to clear height for single exhaust point

layer temperature can be replaced using Equation 51.34 (assuming adiabatic conditions) to express the minimum smoke layer depth in terms of the heat release rate and clear height as indicated in Fig. 51.21. For a single extract point, the minimum smoke layer depth is slightly less than 40 % of the clear height.

Makeup Air Supply

The makeup air supplied to the atrium should be

- Uncontaminated
- Introduced below the smoke layer
- Introduced at a slow velocity
- Supplied at a rate less than the required exhaust rate

Air that is not contaminated by smoke can be provided by locating intakes for the makeup air remote from the smoke exhaust discharge, preventing smoke feedback. To address the potential for smoke being introduced into the makeup air supply, a smoke detector should be provided to shut down the makeup air supply system. Selection of a smoke detector for this application should consider the operating conditions, range of temperatures, and installation within a duct.

All makeup air should be provided below the smoke layer interface. Any makeup air provided above the smoke layer interface merely adds mass to the smoke layer, which must be added to the required capacity of the smoke exhaust to prevent an increase in the smoke layer depth. If introduced near the smoke layer interface, the makeup air may increase the amount of mixing of clean air with the smoke to further add to the smoke layer.

Makeup air should be provided at a slow velocity so that the plume, fire, and smoke layer are not adversely affected. Makeup air supplied at a rapid velocity near the plume may deflect the plume to enhance the entrainment rate, thereby increasing the rate of smoke production. In addition, the burning rate of the fire may be increased by makeup air provided at an excessive velocity. Because the entrainment process induces an air velocity of approximately 1 m/s, the maximum makeup air velocity in the vicinity of the plume is often recommended to be 1 m/s. Because of the diffusion of air once past the diffuser, the makeup air velocity at the diffuser may be greater than 1 m/s.

Finally, the mass rate of makeup air supplied must be less than that being exhausted. Failure to follow this guideline may lead to the atrium being pressurized relative to the communicating spaces. Being at a positive pressure, smoke movement will be forced through any unprotected openings in physical barriers into the communicating spaces.

Limited Fuel

In some cases smoke management objectives may be fulfilled without a dedicated smoke control system due to the intrinsic qualities of the atrium. The intrinsic qualities of the atrium include parameters, such as the composition and quantity of fuel and geometry of the atrium. As an example, a limited amount of fuel may be present that is unable to sustain a fire for a sufficient period of time to create conditions beyond the allowable limits. The amount of fuel consumed during the time period of interest depends on whether the fire is steady or unsteady. In the case of a steady fire, the fuel mass consumed in a given period of time is determined as

$$\dot{m}_f = \frac{\dot{Q}_t}{H_c} \tag{51.56}$$

Alternatively, for an unsteady, t^2 profile fire, the fuel mass consumed during a given period of time is given as

$$\dot{m}_f = 333\frac{t^3}{H_c t_g^2} \tag{51.57}$$

When analyzing the inherent ability of the atrium to fulfill the smoke management design goals, the time period should relate either to the performance of a fire protection system or to the development of smoke layer conditions in excess of acceptable levels. For example, in life safety–oriented designs, the time period may be either that required for evacuation, or for untenable conditions to be generated, whichever is less.

Opposed Airflow

Opposed airflow refers to systems where airflow is provided in a direction opposite to the undesired direction of smoke movement. Opposed airflow may be used in lieu of physical barriers to prevent smoke spread from one space to another (i.e., between the communicating space and the atrium). Opposed airflow limits smoke flow by countering the momentum of the smoke attempting to enter the adjoining space. A minimum airflow velocity at all points of the opening must be provided in order to prevent smoke migration through the opening. Empirical correlations to estimate the minimum average velocity for the entire opening are available, based on limited experimental data [78]. The calculated average velocity is greater than the actual minimum velocity required at an opening to oppose smoke propagation to insure that the minimum critical velocity is achieved at all points, considering the effects of turbulence caused by the edges and corners of the opening.

The minimum average velocity to oppose smoke originating in the communicating space is evaluated using Equation 51.59.

$$v_e = 0.64\sqrt{\frac{gH(T_s - T_o)}{T_s}} \tag{51.58}$$

Alternatively, if the smoke at the opening is part of a rising plume that is rising along the side of the atrium wall, then Equation 51.60 is applicable.

$$v_e = 0.057\left(\frac{\dot{Q}}{z}\right)^{1/3} \tag{51.59}$$

The opposed airflow velocity should not exceed 1 m/s. Above that limit, the airflow velocity may deflect the plume away from the wall, making more plume surface area available for entrainment. The increased area for entrainment will enhance the smoke generation rate. Consequently, the problem of propagation to the communicating space may be solved by an excessive average velocity; however, other problems may be created by the increased smoke production rate and a possible increase in the depth of the smoke layer in the atrium. The volumetric capacity of the mechanical equipment required to deliver the necessary velocity for opposed airflow can be approximated as

$$V_{\text{oa}} = A_o v_e \tag{51.60}$$

If several openings are protected with the opposed airflow approach using the same

mechanical equipment, the cross-sectional area should be the sum of the areas for all of the openings. The opposed airflow technique may be infeasible due to the substantial amount of airflow capacity required to protect numerous openings having a large total area.

Where opposed airflow is utilized, the impact of the volume of air being introduced into the space with the fire must be assessed. For example, if the airflow is directed into the atrium and smoke exhaust equipment is also provided to maintain a constant position of the smoke layer interface in the atrium, then all of the additional air used for opposed airflow must also be exhausted. The additional air can be accounted for by increasing the required mass rate of exhaust in the atrium by the amount used for the opposed airflow. The additional air being exhausted will also affect the qualities of the smoke layer within the atrium (see Equations 51.34, 51.38, and 51.40). The smoke layer temperature, T_s(K), can be determined using Equation 51.61, based on an analysis included elsewhere [3].

$$T = 293 + \left[0.0018 + 0.072\dot{Q}_c^{-2/3} z^{5/3} + \frac{712 A_o \sqrt{H(T-293)}}{\dot{Q}_c T^{3/2}}\right]^{-1} \quad (51.61)$$

Equation 51.61 must be applied iteratively to determine the resulting smoke layer temperature. In cases with large clear heights, the temperature of the air used for the opposed airflow strategy will be virtually equal to the temperature of the smoke layer to permit the addition of volumetric rates of air rather than mass rates.

Alternatively, if airflow is directed from the atrium into a communicating space, the communicating space must also be exhausted, otherwise the communicating space will become positively pressurized.

Example 8 Considering the atrium from Example 5. There are five 5-m-wide × 2.5-m-high openings to the communicating space. The bottom of the openings is 30 m above the floor of the atrium. Considering a 5000 kW fire in the center of the floor of the atrium, determine the following:

1. Minimum airflow velocity required for opposed airflow
2. Volumetric rate of air supply for opposed airflow
3. Capacity of the exhaust fans in the atrium to maintain the smoke layer interface at an elevation 25 m above floor level and also to accommodate the additional air from the opposed airflow approach

Solution The minimum opposed airflow velocity can be determined using Equation 51.60. However, the temperature of the smoke layer, T, is unknown. Thus, Equation 51.61 must be applied first. Solving iteratively, T is approximately 305 K. The minimum airflow velocity is 0.20 m/s. The volumetric supply capacity for the opposed airflow strategy for all five openings is 12.5 m^3/s. The associated mass flow rate is 15.0 kg/s.

Without the opposed airflow, the mass rate of smoke exhaust required to maintain the smoke layer interface height in the atrium at a height of 25 m is determined using Equation 51.27 to be 236 kg/s. Thus, the combined mass exhaust rate necessary is 251 kg/s. This mass flow rate corresponds to a volumetric rate of 209 m^3/s.

As a practical issue, this exhaust rate should be compared to that required to keep the smoke layer interface above the top of the openings (i.e., 32.5 m above floor level). Based on Equations 51.27 and 51.29, the required volumetric exhaust rate is 362 kg/s. Thus, in this situation, the combined exhaust rate with the opposed airflow strategy is less than that associated with the strategy to keep the smoke layer interface above the opening.

Nomenclature

A	Cross-sectional area of the atrium (m^2)
A_o	Cross-sectional area of opening (m^2)
b	Distance from the store opening to the balcony edge (m)

C_{CO}	Volumetric concentration of carbon monoxide (ppm)
c_p	Specific heat (kJ/kg-K)
D	Optical density per unit pathlength (m^{-1})
D_m	Mass optical density (m^2/kg)
d	Plume diameter (based on excess temperature) (m)
d_o	Diameter of fire (m)
f_{CO}	Yield fraction of CO (kg_{CO}/kg_{fuel})
f_i	Yield fraction of species i (kg of species i per kg of fuel consumed)
g	Gravitational acceleration (9.8 m/s^2)
H	Height of ceiling above top of fuel surface (m)
H_b	Height of balcony above top of fuel surface (m)
H_c	Heat of combustion (kJ/kg)
$H_{c,conv}$	Convective heat of combustion (kJ/kg)
h	Enthalpy
K	Constant, depending on target being viewed (e.g., = 6 for lighted signs)[3]
k	Thermal conductivity (W/m·K)
k_v	Volumetric entrainment constant (0.065 $m^{4/3}$ kW $\cdot^{-1/3}\cdot$ s^{-1})
L	Width of balcony spill plume (m)
l	Characteristic length (m)
MW_i	Molecular weight of species i (kg)
M_{CO}	Molecular weight of carbon monoxide (28 kg)
M_{air}	Molecular weight of air (29 kg)
m_u	Mass of upper smoke layer (kg)
$\dot{m}$	Mass entrainment rate in plume (kg/s)
m_f	Mass burning rate (kg/s)
Δp	Pressure difference (Pa)
r	Radius (i.e., horizontal distance from plume centerline (m)
Q	$= \frac{1055}{t_g^2}\frac{t^3}{3}$ for t^2 fires (kJ)
$Q=$	$\dot{Q}\ t$ for steady fires (kJ)
$Q_o=$	$\rho_o c_p T_o A(H–z)$ (kJ)
$\dot{Q}$	Heat release rate of fire (kW)
$\dot{Q}_c$	Convective portion of heat release rate of fire (kW)
T_c	Temperature at plume centerline (K)
T	Temperature (K)
ΔT_{ad}	Temperature difference between smoke layer and ambient air (°C)
ΔT_o	Prefire temperature change from floor to ceiling of the ambient air (°C)
t	Time (s)
t_{cj}	Ceiling jet transport lag (s)
t_g	Growth time (s)
t_{pl}	Plume transport lag (s)
V	Volumetric flow rate (m^3/s)
V_{oa}	Volumetric capacity required for opposed air-flow (m^3/s)
V_u	Volume of upper layer (m^3)
v	Characteristic velocity (m/s)
v_e	Opposed airflow velocity (m/s)
w	Width of the balcony opening from the area of origin (m)
x	Position (m)
Y_{CO}	Mass fraction of CO (kg of species CO per kg of smoke)
Y_i	Mass fraction of gas species i (kg of species i per kg of smoke)
z	Clear height, position of smoke layer interface above the top of fuel surface (m)
z_b	position of smoke layer interface above top of balcony (m)
z_f	Limiting height above fuel (m)
z_m	Maximum rise of plume (m)
z_o	Virtual origin of plume (m)
χ_a	Combustion efficiency
χ_l	Heat loss fraction from smoke to enclosure
ρ	Density (kg/m^3)

Subscripts

F	Full-scale building
m	Small-scale model
o	Ambient air
w	Wall, ceiling, or floor of enclosure

References

1. NFPA 92, *Standard for Smoke-Control Systems,* National Fire Protection Association, Quincy, MA (2012).***was 92A
2. J.H. Klote, J.A. Milke, P.G. Turnbull, A. Kashef, and M.J. Ferreira, *Handbook of Smoke Control Engineering,* ASHRAE, Atlanta (2012).

3. T. Jin, "Irritating Effects of Fire Smoke on Visibility," *Fire Science and Technology,* 5, 1 (1985).
4. J. Morehart, "Sprinklers in the NIH Atrium: How Did They React During the Fire Last May?" *Fire Journal,* 83, pp. 56–57 (1989).
5. NFPA 75, *Standard for the Protection of Information Technology Equipment,* National Fire Protection Association, Quincy, MA (2009).
6. R.D. Peacock and E. Braun, "Fire Tests of Amtrak Passenger Rail Vehicle Interiors," *NBS Technical Note 1193,* National Bureau of Standards, Gaithersburg, MD (1984).
7. V. Babrauskas, "A Laboratory Flammability Test for Institutional Mattresses," *Fire Journal,* 72, 93, pp. 35–40 (1981).
8. S.W. Harpe, T.E. Waterman, and W.S. Christian, "Detector Sensitivity and Siting Requirements for Dwellings, Phase 2, Part 2 'Indiana Dunes Tests,'" Report No. PB-263882, National Bureau of Standards, Gaithersburg, MD (1977).
9. Milke, J.A., Hugue, D.E., Hoskins, B.L., and Carroll J.P., "Tenability Analyses in Performance-Based Design," *Fire Protection Engineering*, 28, 50-56 (2005),
10. J.L. Bryan, "Damageability of Buildings, Contents, and Personnel from Exposure to Fire," *Fire Safety Journal,* 11, pp. 15–32 (1984).
11. J.A. Milke and J.H. Klote, "Smoke Management in Large Spaces in Buildings," Building Control Commission of Victoria and The Broken Hill Proprietary Company Limited, Melbourne, Australia (1998).
12. J.G. Quintiere, "Scaling Applications in Fire Research," *Fire Safety Journal,* 15, pp. 3–29 (1989).
13. F.W. Mowrer, "Lag Times Associated with Fire Detection and Suppression," *Fire Technology,* 26, 3, pp. 244–265 (1990).
14. J.S. Newman, "Principles for Fire Detection," *Fire Technology,* 24, 2, pp. 116–127 (1988).
15. J.A. Milke, "Smoke Management for Covered Malls and Atria," *Fire Technology,* 26, 3, pp. 223–243 (1990).
16. G. Heskestad and M.A. Delichatsios, "Environments of Fire Detectors—Phase I: Effect of Fire Size, Ceiling Height, and Materials," *Vol. I—Measurements (NBS-GCR-77-86), Vol. II—Analysis (NBS-GCR-77-95),* National Bureau of Standards, Gaithersburg, MD (1977).
17. B.R. Morton, Sir Geoffrey Taylor, and J.S. Turner, "Turbulent Gravitational Convection from Maintained and Instantaneous Sources," in *Proceedings of Royal Society A,* 234, pp. 1–23, London (1956).
18. G. Mulholland, T. Handa, O. Sugawa, and H. Yamamoto, "Smoke Filling in an Enclosure," *Paper 81-HT-8,* The American Society of Mechanical Engineers, New York (1981).
19. L.Y. Cooper, M. Harkleroad, J. Quintiere, and W. Rinkinen, "An Experimental Study of Upper Hot Layer Stratification in Full-Scale Multiroom Fire Scenarios," *Paper 81-HT-9,* The American Society of Mechanical Engineers, New York (1981).
20. G. Heskestad, Letter to the Editor, *Fire Technology,* 27, 2, pp. 174–185 (1991).
21. T. Yamana and T. Tanaka, "Smoke Control in Large Spaces (Part 2—Smoke Control Experiments in a Large-Scale Space)," *Fire Science and Technology,* 5, 1, pp. 41–54 (1985).
22. G.D. Lougheed, Personal Communication, National Research Council of Canada (Mar. 20, 1991).
23. S.P. Nowlen, "Enclosure Environment Characterization Testing for the Baseline Validation of Computer Fire Simulation Codes," *NUREG/ CR-4681, SAND 86–1296,* Sandia National Laboratories, Albuquerque, NM (1987).
24. J.A. Sharry, "An Atrium Fire," *Fire Journal,* 67, 6, pp. 39–41 (1973).
25. J. Lathrop, "Atrium Fire Proves Difficult to Ventilate," *Fire Journal,* 73, 1, pp. 30–31 (1979).
26. D.M. McGrail, "Denver's Polo Club Condo Fire: Atrium Turns High-Rise Chimney," *Fire Engineering,* pp. 67–74 (1992).
27. G. Heskestad, "Engineering Relations for Fire Plumes," *SFPE TR 82-8,* Society of Fire Protection Engineers, Boston (1982).
28. C. Beyler, "Fire Plumes and Ceiling Jets," *Fire Safety Journal,* 11, pp. 53–76 (1986).
29. R.L. Alpert and E.J. Ward, "Evaluation of Unsprinklered Fire Hazards," *Fire Safety Journal,* 7, pp. 127–143 (1984).
30. F.W. Mowrer and B. Williamson, "Estimating Room Temperatures from Fires along Walls and in Corners," *Fire Technology,* 23, 2, pp. 133–145 (1987).
31. Harrison, R., "Entrainment of Air Into Thermal Spill Plumes," PhD Dissertation, University of Canterbury, New Zealand (2009).
32. Lougheed, GD., McCartney, C.J. and Gibbs, E., "Balcony Spill Plumes Final Report, RP-1247, ASHRAE, Atlanta (2007).
33. Lim, J.M.K., "Numerical Modeling of Balcony Spill Plumes Using Fire Dynamics Simulator (FDS)," MS Thesis, University of Maryland (2010).
34. M. Law, "A Note on Smoke Plumes from Fires in Multi-Level Shopping Malls," *Fire Safety Journal,* 10, pp. 197–202 (1986).
35. H.P. Morgan and N.R. Marshall, "Smoke Control Measures in a Covered Two-Story Shopping Mall Having Balconies and Pedestrian Walkways," *BRE CP11/79,* Fire Research Station, Borehamwood, England (1979).
36. W.D. Walton, "ASET-B: A Room Fire Program for Personal Computers," *NBSIR 85-3144,* National Bureau of Standards, Gaithersburg, MD (1985).
37. Lincolne Scott Australia Pty Ltd., *Jupiters Casino—Report on Atrium Smoke Tests,* Lincolne Scott Australia Pty Ltd., Toowong, Australia (1986).

38. G.O. Hansell and H.P. Morgan, "Smoke Control in Atrium Buildings Using Depressurization," *PD 66/88,* Fire Research Station, Borehamwood, UK (1988).
39. R.A. Waters, "Stansted Terminal Building and Early Atrium Studies," *Journal of Fire Protection Engineering,* 1, 2, pp. 63–76 (1989).
40. G. Heskestad, "Similarity Relations for the Initial Convective Flow Generated by Fire," *Paper 72-WA/HT-17,* American Society of Mechanical Engineers, New York (1972).
41. T. Jin, "Visibility Through Fire Smoke (Part 2)," *Report of the Fire Research Institute of Japan, Nos. 33, 31,* Tokyo (1971).
42. J.G. Quintiere, "An Assessment of Correlations Between Laboratory and Full-Scale Experiments for the FAA Aircraft Fire Safety Program, Part 1: Smoke," *NBSIR 82-2508,* National Bureau of Standards, Gaithersburg, MD (1982).
43. G. Heskestad, "Hazard Evaluation," submitted to NFPA Task Group on Smoke Management of Atria, Covered Malls, and Large Spaces, unpublished manuscript (1988).
44. G.D. Lougheed, "Probability of Occurrence and Expected Size of Shielded Fires in Sprinklered Building; Phase 2, Full-Scale Fire Tests," National Research Council of Canada, Ottawa (1997).
45. NFPA 204, *Standard for Smoke and Heat Venting,* National Fore Protection Association, Quincy, MA (2012).
46. C.L. Beyler and L.Y. Cooper, "Interaction of Sprinklers with Smoke Vents," *Fire Technology,* 37, 1, pp. 9–36 (2001).
47. M.L. Bullen, "The Effect of a Sprinkler on the Stability of a Smoke Layer beneath a Ceiling," *Fire Research Note No. 1016,* Department of the Environment and Fire Officers' Committee, Joint Fire Research Organization, Watford, UK (1974).
48. M.L. Bullen, "The Effect of a Sprinkler on the Stability of a Smoke Layer beneath a Ceiling," *Fire Technology,* 13, 1, pp. 21–34 (1977).
49. R.L. Alpert, "Calculated Interaction of Sprays with Large-Scale Buoyant Flows," *Journal of Heat Transfer,* 106, pp. 310–317 (1984).
50. A.J. Gardiner, *First Report on the Interaction between Sprinkler Sprays and the Thermally Buoyant Layers of Gases from Fires,* South Bank Polytechnic, London (1985).
51. A.J. Gardiner, *Second Report on the Interaction between Sprinkler Sprays and the Thermally Buoyant Layers of Gases from Fires,* South Bank Polytechnic, London (1986).
52. A.J. Gardiner, *Third Report on the Interaction between Sprinkler Sprays and the Thermally Buoyant Layers of Gases from Fires,* South Bank Polytechnic, London (1988).
53. A.J. Gardiner, *Fourth Report on the Interaction between Sprinkler Sprays and the Thermally Buoyant Layers of Gases from Fires,* South Bank Polytechnic, London (1988).
54. L.A. Jackman, *Second Report on the Interaction between Sprinkler Sprays and the Thermally Buoyant Layers of Gases from Fires,* South Bank Polytechnic, London (1990).
55. L.A. Jackman, *Third Report on the Interaction between Sprinkler Sprays and the Thermally Buoyant Layers of Gases from Fires,* South Bank Polytechnic, London (1991).
56. L.A. Jackman, P.F. Nolan, A.J. Gardiner, and H.P. Morgan, *Mathematical Model of the Interaction of Sprinkler Spray Drops with Fire Gases,* South Bank University, London, Swedish Fire Research Board, and National Institute of Standards and Technology (NIST), Fire Suppression Research, First International Conference on Fire Suppression Research, May 5–8, 1992, Stockholm, Sweden, (V. Sjolin, D.D. Evans, and N.H. Jason, eds.), pp. 209–227 (1992).
57. G. Heskestad, "Sprinkler/Hot Layer Interaction," *NIST-GCR-91-590,* National Institute of Standards and Technology (NIST), Gaithersburg, MD (1991).
58. L.Y. Cooper, "The Interaction of an Isolated Sprinkler Spray and a Two-Layer Compartment Fire Environment. Phenomena and Model Simulations," *Fire Safety Journal,* 25, 2, pp. 89–107 (1995).
59. L.Y. Cooper, "The Interaction of an Isolated Sprinkler Spray and a Two-Layer Compartment Fire Environment," *International Journal Heat and Mass Transfer,* 38, 4, pp. 679–690 (1995).
60. P.L. Hinkley, "Work by the Fire Research Station on the Control of Smoke in Covered Shopping Centers," *BRE Paper CP 83/75,* Building Research Establishment (BRE), Fire Research Station (FRS), London (1975).
61. A.J.M. Heselden, "The Interaction of Sprinklers and Fire Venting," *Fire Surveyor,* 11, 5, pp. 13–28 (1982).
62. G. Holmstedt, "Sprinkler and Fire Venting Interaction," *Literature Survey on Modeling Approaches and Experiments Available and Recommendations for Further Studies, 92178 AR GH/AB,* Swedish Fire Research Board, Stockholm, Sweden (1992).
63. B. Persson and H. Ingason, "Modeling of Interaction between Sprinklers and Fire Vents," *SP Report 1996:32,* Swedish National Testing and Research Institute, Sweden (1996).
64. L.Y. Cooper, "LAVENTS—A Computer Program to Model the Interaction between Sprinklers, Smoke Layers, and Smoke Vents," presented at the *International Conference on Smoke Ventilation and Sprinklers—Aspects of Combined Use,* Fire Research Station, Borehamwood, UK (1992).
65. K.B. McGrattan, A. Hamins, D.W. Stroup, "Sprinkler, Smoke and Heat Vent, Draft Curtain Interaction—Large-Scale Experiments and Model Development," *NISTIR 6196,* National Institute of Standards and Technology (NIST), Gaithersburg, MD (1998).
66. K.B. McGrattan, H.R. Baum, and R.G. Rehm, "Large Eddy Simulations of Smoke Movement," *Fire Safety Journal,* 30, pp. 161–178 (1998).

67. K.B. McGrattan and D.W. Stroup, "Sprinkler, Vent and Draft Curtain Interaction: Experiment and Computer Simulation," *National Institute of Standards and Technology (NIST),* Gaithersburg, MD (1997).
68. K.B. McGrattan and D.W. Stroup, "Large Eddy Simulations of Sprinkler, Vent and Draft Curtain Performance," *Fire Suppression and Detection Research Application, Symposium, Research and Practice: Bridging the Gap, Proceedings,* National Fire Protection Research Foundation, February 12–14, 1997, Orlando, FL, pp. 59–68 (1997).
69. H. Touvinen, "Validation of Ceiling Jet Flows in a Large Corridor with Vents Using the CFD Code JASMINE," *Fire Technology,* 32, 1, pp. 25–49 (1996).
70. H. Touvinen and L.Y. Cooper, "Validation of Ceiling Jet Flows in a Large Corridor with Vents Using the CFD Code JASMINE: Errata and Additional Remarks," *Fire Technology,* 33, 2, pp. 183–186 (1997).
71. R.N. Mawhinney, E.R. Galea, and M.K. Patel, "Euler-Lagrange Modeling of Fire/Sprinkler Interactions," *Fire Safety Science—Proceedings of the Fifth International Symposium,* International Association of Fire Safety Science (IAFSS), Australia, p. 1336 (1997).
72. W.K. Chow and A.C. Tang, "Experimental Studies on Sprinkler Water Spray Smoke Layer Interaction," *Journal of Applied Fire Science,* 4, 3, pp. 171–184 (1994–95).
73. G. Heskestad, "Note on Maximum Rise of Fire Plumes in Temperature-Stratified Ambients," *Fire Safety Journal,* 15, pp. 271–276 (1989).
74. M. Dillon, "Acceptance Testing and Techniques," presented at *The Roundtable on Fire Safety in Atriums—Are the Codes Meeting the Challenge?,* Washington, DC (1988).
75. T. Handa and O. Sugawa, "Flow Behavior of Plume from Growing Fire Source in High Ceiling Enclosure," *Journal of Fire and Flammability,* 12, 1, pp. 31–50 (1981).
76. G. Heskestad, "Fire Plume Entrainment and Related Problems in Venting of Fire and Smoke from Large Open Spaces," submitted to NFPA Task Group on Smoke Management of Atria, Covered Malls, and Large Spaces, unpublished manuscript (1987).
77. G.D. Lougheed and G.V. Hadjisophocleous, "Investigation of Atrium Exhaust Effectiveness," *ASHRAE Transactions,* 103, 2 (1997).
78. G. Heskestad, "Inflow of Air Required at Wall and Ceiling Apertures to Prevent Escape of Fire Smoke," *FMRC J. I. OQ4E4.RU,* Factory Mutual Research Corporation, Norwood, MA (1989).

James A. Milke is a professor and chair in the Department of Fire Protection Engineering at the University of Maryland. His recent research activities have included assessing the performance of smoke control systems in fires.

آموزشگاه ادوفایر
EDUFIRE

ویدیو – انیمیشن های اطفا، اعلام حریق، تهویه وتخلیه دود (رایگان)

برای مشاهده هر یک از ویدیوهای زیر کافیست بر روی عنوان آن آموزش کلیک نمایید تا به صفحه ویدیو و آموزش آن عنوان هدایت شوید.

انیمیشن ویدیو

- اطفا حریق آبی
  - سیستم اطفا لوله خشک اسپرینکلر
  - سیستم اطفا لوله تر اسپرینکلر
  - سیستم اطفا پیش عملگر
  - سیستم اطفا واترمیست
  - سیستم اطفا سیلابی
- سیستم اطفا فوم
- تجهیزات اطفا حریق - تجهیزات هشدار دهنده
- تجهیزات اطفا حریق- اسپرینکلر
- سیستم اطفا آشپزخانه صنعتی
- سیستم اطفا آیروسل
- سیستم اطفا دستی
- سیستم اطفا گازی
  - سیستم اطفا FM200 , NOVEC, Inert Gas (IG)
  - سیستم اطفا CO_2
- سیستم تهویه و تخلیه دود
- سیستم اعلام حریق
  - آدرس‌پذیر
  - متعارف

تهران . خیابان سعدی شمالی .خیابان مرادی نور . پلاک ۳۱ . واحد ۱
۰۲۱ – ۷۷۶۸۶۹۶۶ – ۰۹۳۵۴۷۴۳۹۱۳
WWW.EDUFIRE.IR

آموزشگاه ادوفایر
EDUFIRE

آموزش استاندارد

- آموزش استاندارد NFPA 13
- آموزش استاندارد NFPA 14
- آموزش استاندارد NFPA 20

آموزش نرم‌افزار

- اتواسپرینک
- پایروسیم
- پث‌فایندر

دانلود استاندارد

- ترجمه استاندارد NFPA 30,14,13,10
- تمامی استانداردهای NFPA & FM
- ترجمه استاندارد NFPA 1037

محصولات

- اتواسپرینک ۲۰۱۳ و ۲۰۱۹ به زبان فارسی برای اولین بار در ایران
- آلارم کد ۲۰۱۹ به زبان فارسی برای اولین بار در ایران
- اطفا حریق آبی
- پایپ‌نت (ماژول اسپرینکلر)
- کانتم
- اعلان حریق

دوره‌های حضوری

- آموزش اتواسپرینک
- آموزش آلارم‌کد
- آموزش پایروسیم
- آموزش کانتم + اگزاست
- آموزش اطفا آبی +پمپ + بازدید از کارگاه
- آموزش اطفا گازی
- آموزش اطفا فوم
- آموزش مبحث سوم مقررات ملی
- آموزش اعلام حریق F&G
- آموزش اعلام حریق آدرس‌پذیر
- آموزش اعلام حریق متعارف
- دوره آمادگی آزمون آتش‌نشانی (برق، مکانیک، عمران، معماری)

تهران . خیابان سعدی شمالی .خیابان مرادی نور . پلاک ۳۱ . واحد ۱
۰۲۱ – ۷۷۶۸۶۹۶۶ – ۰۹۳۵۴۷۴۳۹۱۳
WWW.EDUFIRE.IR

آموزشگاه ادوفایر
EDUFIRE

تهران . خیابان سعدی شمالی .خیابان مرادی نور . پلاک ۳۱ . واحد ۱
۰۲۱ – ۷۷۶۸۶۹۶۶ – ۰۹۳۵۴۷۴۳۹۱۳
WWW.EDUFIRE.IR

آموزشگاه ادوفایر
EDUFIRE

تهران . خیابان سعدی شمالی .خیابان مرادی نور . پلاک ۳۱ . واحد ۱
۰۹۳۵۴۷۴۳۹۱۳ - ۷۷۶۸۶۹۶۶ - ۰۲۱
WWW.EDUFIRE.IR